Supplemental Figures and Tables for:

Failed immune responses across multiple pathologies share pan-tumor and circulating lymphocytic targets

Includes Supplemental Figures:

Includes Supplemental Tables:

Figure S1

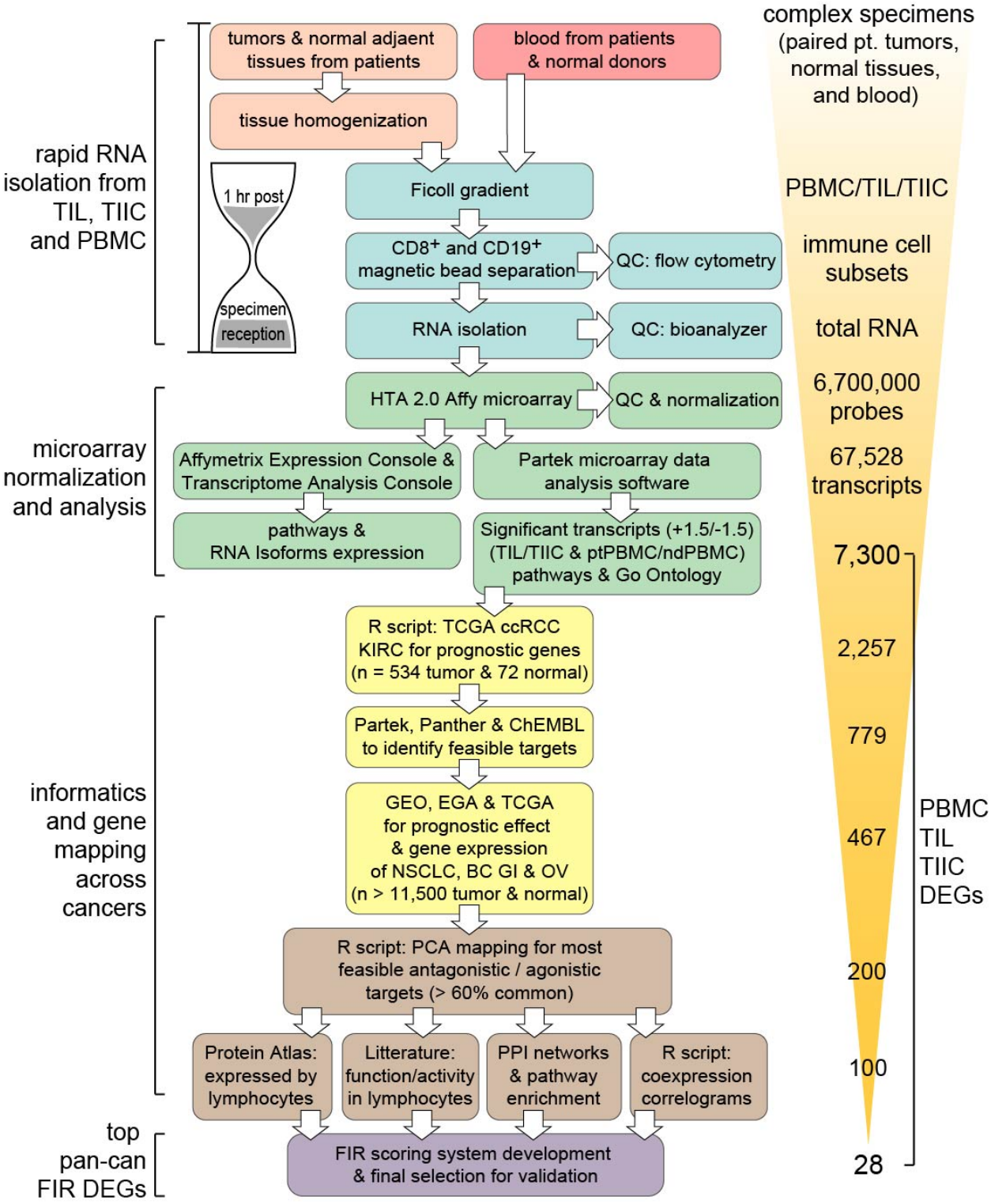
complex specimens
(paired pt. tumors, normal tissues, and blood)
rapid RNA isolation from TIL, TIIC and PBMC
tumors & normal adjaent tissues from patients
blood from patients & normal donors
tissue homogenization
1 hr post
specimen reception
Ficoll gradient
PBMC/TIL/TIIC
CD8+ and CD19+ magnetic bead separation
QC: flow cytometry
immune cell subsets
RNA isolation
QC: bioanalyzer
total RNA
HTA 2.0 Affy microarray
QC & normalization
6,700,000 probes
microarray normalization and analysis
Affymetrix Expression Console & Transcriptome Analysis Console
Partek microarray data analysis software
67,528 transcripts
pathways & RNA Isoforms expression
Significant transcripts (+1.5/-1.5) (TIL/TIIC & ptPBMC/ndPBMC) pathways & Go Ontology
7,300
R script: TCGA ccRCC KIRC for prognostic genes (n = 534 tumor & 72 normal)
2,257
Partek, Panther & ChEMBL to identify feasible targets
779
informatics and gene mapping across cancers
GEO, EGA & TCGA for prognostic effect & gene expression of NSCLC, BC GI & OV (n > 11,500 tumor & normal)
467
PBMC TIL TIIC DEGs
R script: PCA mapping for most feasible antagonistic / agonistic targets (> 60% common)
200
Protein Atlas: expressed by lymphocytes
Litterature: function/activity in lymphocytes
PPI networks & pathway enrichment
R script: coexpression correlograms
100
top pan-can FIR DEGs
FIR scoring system development & final selection for validation
28

Supplemental Figure S1. Full schematic pan-cancer discovery pipeline. Pan-cancer discovery pipeline permitting the refining of >7,300 DEGs identified from training ccRCC cohort, down to ~30 for validation on new ccRCC cohort, as first identified by microarrays performed on paired patient $CD8^+$ and $CD19^+$ TIL and TIL-B, TIIC, and ptPBL, and matched cdPBL. Tumors, normal adjacent tissues and blood are simultaneously received, and used for rapid (~1hr) isolation of immune cell subsets via tissue homogenizing followed by Ficoll gradient and magnetic bead separation. Quality tested RNA is amplified and applied to comprehensive microarray profiling. Gene expression profiles are normalized and DEGs are identified by comparing expression in TIL relative to TIIC, and ptPBL relative to cdPBL (n = 5; fold 1.5; $P < 0.05$). Algorithms designed to probe The Cancer Genome Atlas (TCGA) ccRCC KIRC RNA-Seq and clinical databases (n = 534 tumors; n = 72 normal tissues) were used to identify ccRCC DEGs that had significant effects on patient prognosis. DEGs were refined for most feasible targets by selecting Gene Ontology defined plasma membrane associated proteins (Partek and PANTHER), and proteins having pre-existing targeting compounds for potential drug repurposing (ChEMBL). Additional microarray datasets for lung, breast, gastric and ovarian cancers were probed (n = >11,500 tumors and normal tissues) to refine pan-cancer DEGs that had significant effects on patient prognosis. Principal component analysis (PCA) was used to view most feasible pan-cancer targets (R and R studio). Pan-cancer DEGs were further refined using a four pronged scoring system, taking into account: expression of DEGs by lymphoid and myeloid cells and having modified expression in cancers relative to normal tissues (n = 17 cancers; The Human Protein Atlas), literary evidence that DEGs have been experimentally determined to be expressed in target cells, with existing functional classification in those cell types, and DEG protein-protein interaction (PPI) and coexpression analyses. DEG, differentially expressed genes; TIL, tumor infiltrating lymphocytes; TIIC, normal adjacent tissue infiltrating immune cells; pt, patient; nd, normal donor; PBL, peripheral blood lymphocytes; QC, quality control; HTA, GeneChip Human Transcriptome Array 2.0; TCGA, the Cancer Genome Atlas; GEO, Gene Expression Omnibus; EGA, European Genome-phenome Archive; ccRCC, clear cell renal cell cancer; NSCLC, non-small cell lung cancer; BC, breast cancer; GI gastric cancer; OV, ovarian cancer; PPIs, protein-protein interactions; FIR, failed immune response.

Figure S2

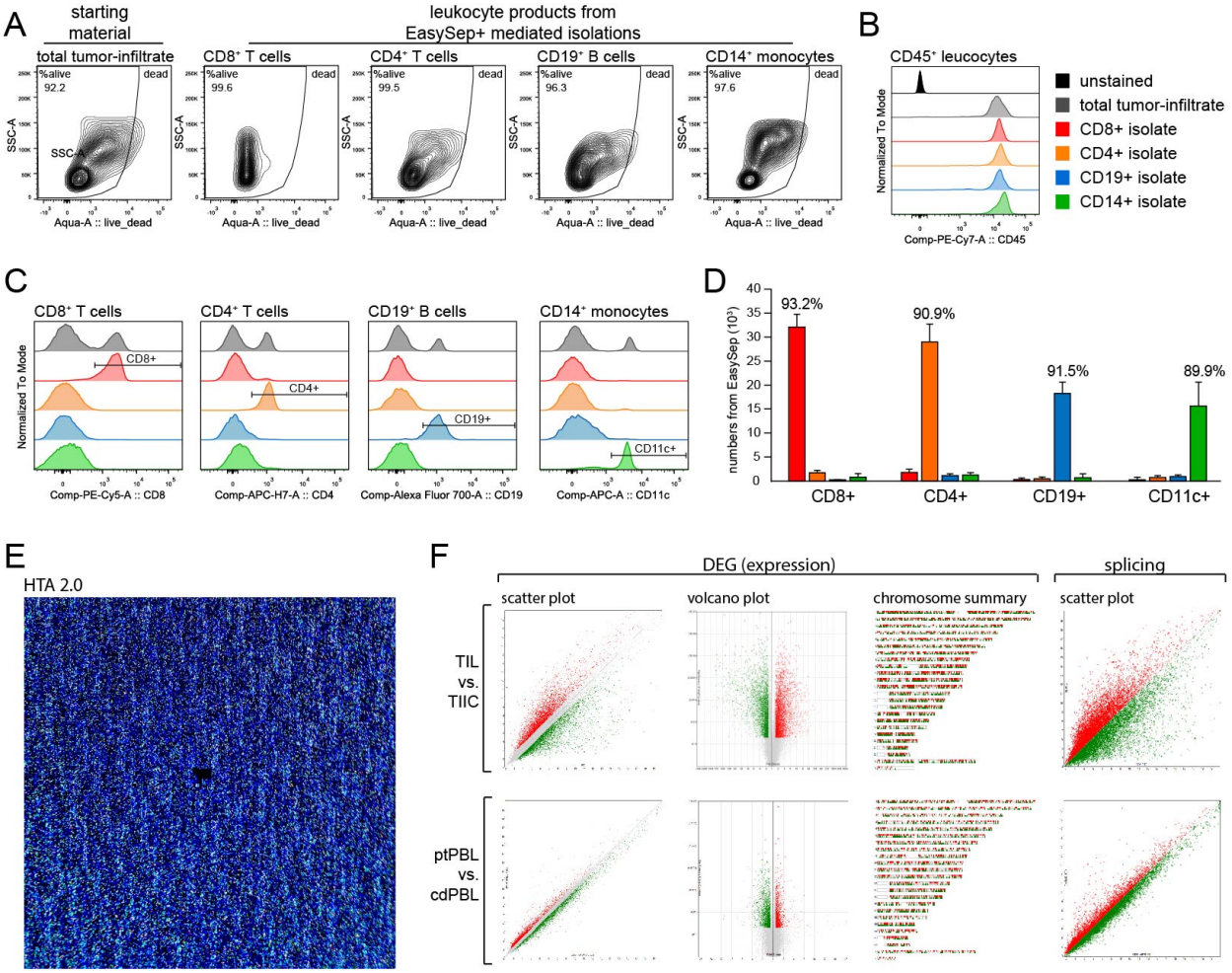
A
starting material
total tumor-infiltrate
leukocyte products from EasySep+ mediated isolations
CD8+ T cells
CD4+ T cells
CD19+ B cells
CD14+ monocytes
%alive
dead
92.2
99.6
99.5
96.3
97.6
SSC-A
Aqua-A :: live_dead
B
CD45+ leucocytes
unstained
total tumor-infiltrate
CD8+ isolate
CD4+ isolate
CD19+ isolate
CD14+ isolate
Normalized To Mode
Comp-PE-Cy7-A :: CD45
C
CD8+ T cells
CD4+ T cells
CD19+ B cells
CD14+ monocytes
CD8+
CD4+
CD19+
CD11c+
Comp-PE-Cy5-A :: CD8
Comp-APC-H7-A :: CD4
Comp-Alexa Fluor 700-A :: CD19
Comp-APC-A :: CD11c
D
numbers from EasySep (10³)
93.2%
90.9%
91.5%
89.9%
CD8+
CD4+
CD19+
CD11c+
E
HTA 2.0
F
DEG (expression)
splicing
scatter plot
volcano plot
chromosome summary
scatter plot
TIL vs. TIIC
ptPBL vs. cdPBL

Supplemental Figure S2. Sample quality control (QC) experiments performed for comprehensive microarrays. QC experiments demonstrate efficient isolation of specific immune subsets from tumors, perfect chip-hybridization and example of paired total $CD8^+$ DEGs resulting from microarrays. Following their magnetic bead-mediated isolation, immune cell subsets were labelled for multi-parametric (M-P) flow cytometry analysis verifying their viabilities, via gating on Aqua LIVE/DEAD assay (Molecular Probes) and quality of their separation from other immune cell subsets isolated by Ficoll gradients. (**A**) Validation of viability of total leukocytes isolated from tumors (left), and $CD8^+$, $CD4^+$, $CD19^+$, and $CD14^+$ tumor infiltrating immune cell subsets isolated using positive selection kits from STEMCELL, as shown by contour plots due to low numbers of isolates. (**B**) Validation that all immune cells isolated from tumors were $CD45^+$ using α-CD45-PE-Cy7 antibody (BD biosciences), using FlowJo v.10 overlay graphs normalized to mode. (**C**) Visual demonstration that positive selection kits were able to rapidly and efficiently separate numerous desired immune cell subsets from tumors, with very little contamination from other immune cell subsets, using clones that are not represented in STEMCELL isolation kits (i.e., α-CD8-PE-Cy5, α-CD4-APC-H7, α-CD19-AF700, α-CD11c-APC; BD biosciences), using FlowJo v.10 overlay graphs normalized to mode (color scheme legend as in (**B**)). Representative percentages of isolates relative to other species examined are shown in (**D**). (**E**) Screen shot example supporting visualization of HTA 2.0 chip hybridization of total amplified $CD8^+$ RNA isolated from TIL (described in methods), where black box in center serves as negative control. (**F**) Examples of $CD8^+$ TIL vs TIIC and ptPBL vs cdPBL DEG expression via scatter and volcano plots, and non-specific chromosome summary segregation patterns of DEG expression, along with splicing/isoform scatter plots of DEGs generated by TAC software (Affymetrix). These demonstrating that TIL have much larger difference in reference to TIIC than ptPBL have in reference to cdPBL. DEG, differentially expressed genes; TIL, tumor infiltrating lymphocytes; TIIC, normal adjacent tissue infiltrating immune cells; pt, patient; nd, normal donor; PBL, peripheral blood lymphocytes.

Figure S3

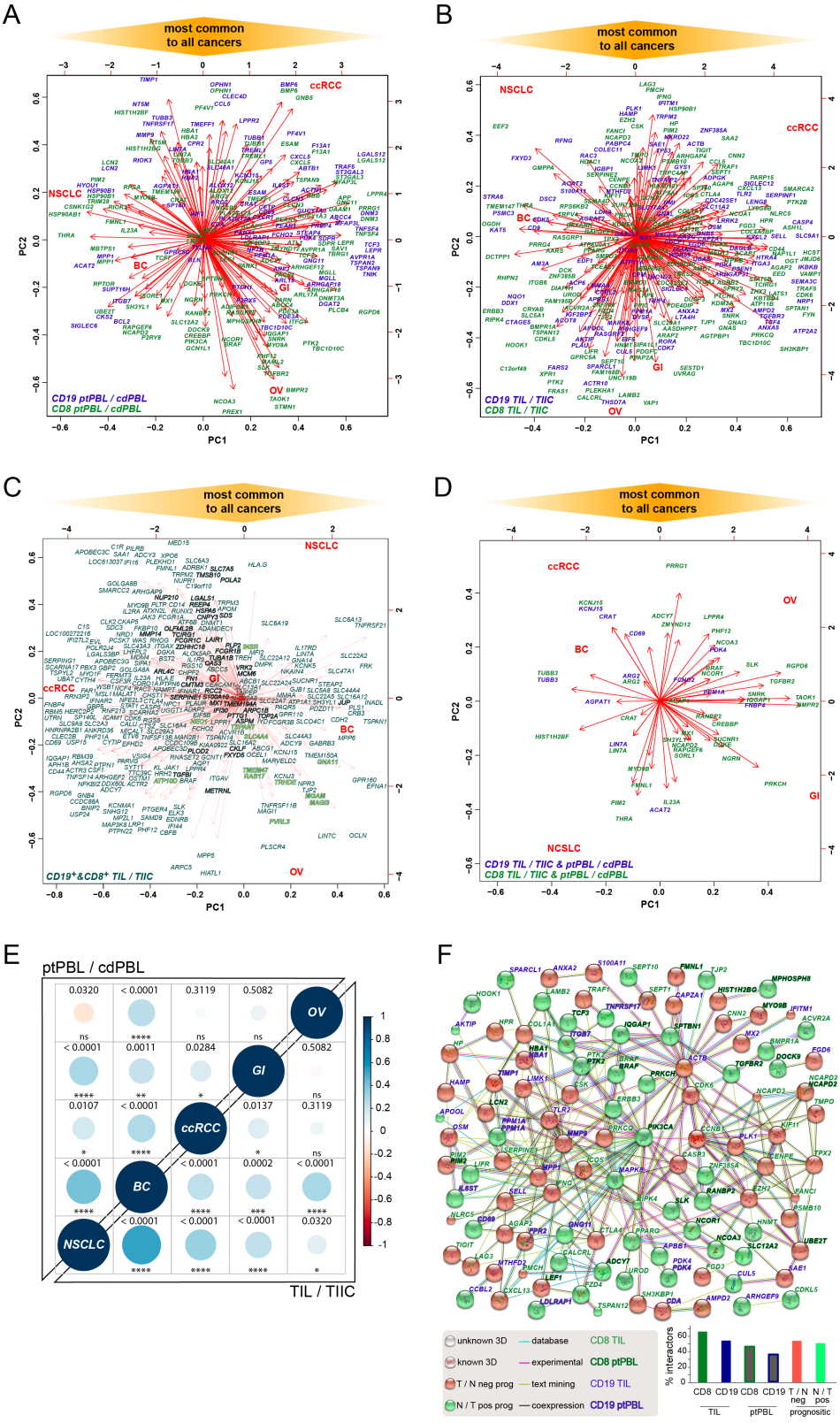
A
most common to all cancers
CD19 ptPBL / cdPBL
CD8 ptPBL / cdPBL
B
most common to all cancers
CD19 TIL / TIIC
CD8 TIL / TIIC
C
most common to all cancers
CD19+&CD8+ TIL / TIIC
D
most common to all cancers
CD19 TIL / TIIC & ptPBL / cdPBL
CD8 TIL / TIIC & ptPBL / cdPBL
E
ptPBL / cdPBL
TIL / TIIC
F
unknown 3D
known 3D
T / N neg prog
N / T pos prog
database
experimental
text mining
coexpression
CD8 TIL
CD8 ptPBL
CD19 TIL
CD19 ptPBL
% interactors
TIL
ptPBL
prognositic

Supplemental Figure S3: Pan-cancer DEG refinery. (**A-C**) Principal component analyses (PCA) of pan-cancer DEGs identified from prognostic and expression scoring across five cancers, common CD8+ (green) or CD19+ (blue) ptPBL (**A**), TIL (**B**) ccRCC identified DEGs at PCA intersects. (**C**) DEGs common to $CD8^+$ TILs and $CD19^+$ TIL-Bs are shown, where dark highlighted gene names represent best antagonistic targets, and green highlighted gene names represent best agonistic targets. (**D**) PCA biplot of DEGs that are commonly identified from ccRCC ptPBL and TIL, where those most common across five cancers are found at PCA intersects. (**E**) Patient PBL and TIL correlograms demonstrating similarities of prognostic effects and gene expression modulation among 483 pan-cancer prognostic biomarkers queried for refinement; demonstrating that DEGs identified from ccRCC ptPBL and TIL have similar results across other cancers: breast cancer (BC), non-small cell lung cancer (NSCLC), gastric cancers (GI), and ovarian cancers (OV) (n > 11,500) (Spearman method, coexpression coefficient ladder on right). (**F**) Protein-protein interaction (PPI) networks between the top 200 DEGs discovered. A high PPI enrichment value (P = 1.85e-10) indicates interactions among these DEGs is very significant relative to proteins drawn from the genome at random; an indicator of biologically connection as groups in defined pathways. Pan-cancer score defined agonistic and antagonistic DEGs are colored red and green, respectively to demonstrate groupings of these two pan-cancer subclasses in unsupervised PPI matrix (String software, v10.5). Bottom graph demonstrates that TIL DEGs are most involved observed in PPI, as are those discovered from CD8+ TIL and ptPBL. TIL, tumor infiltrating lymphocytes; TIIC, normal adjacent tissue infiltrating immune cells; pt, patient; nd, normal donor; PBL, peripheral blood mononuclear cells.

Figure S4

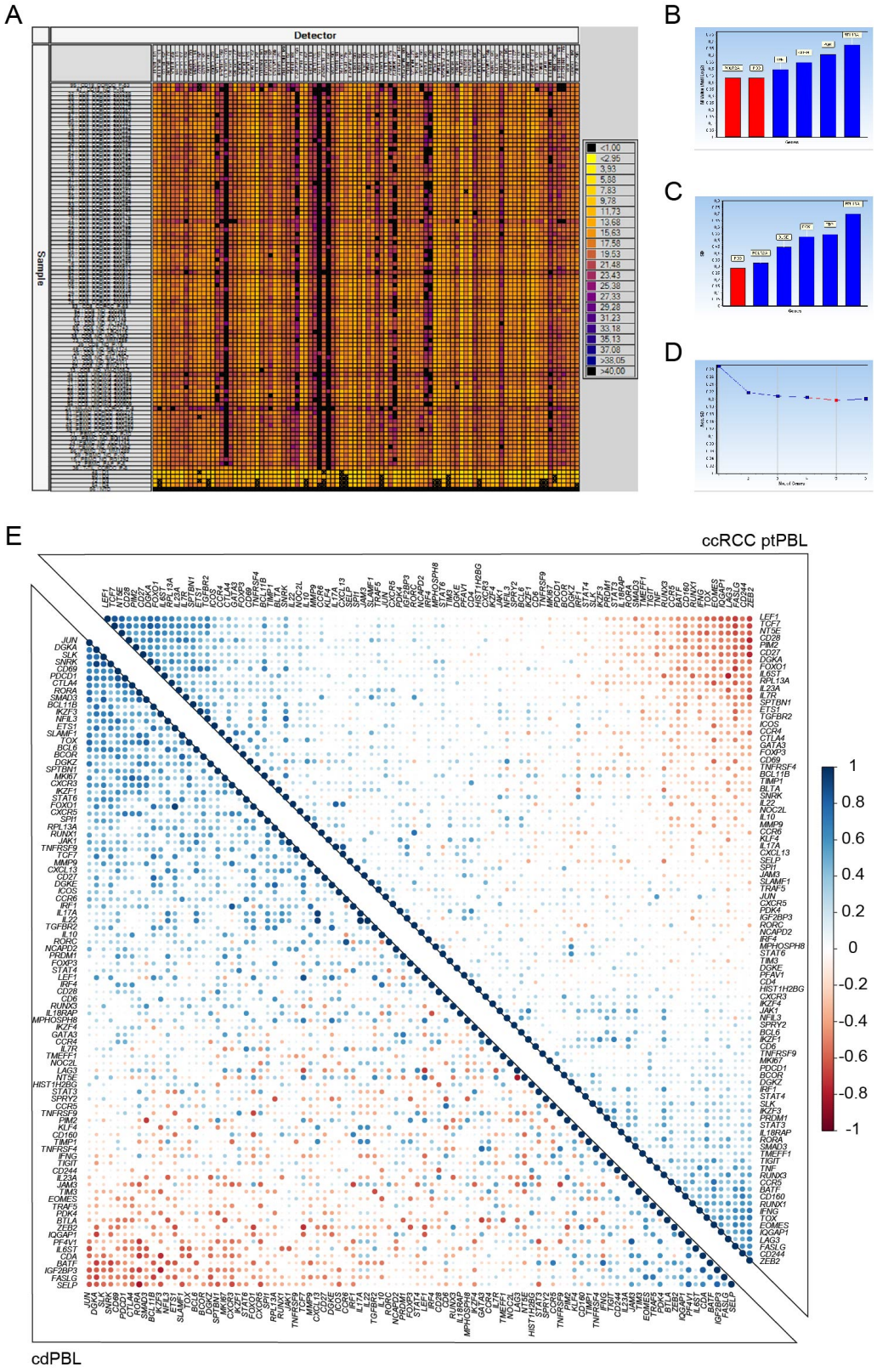
A
Detector
Sample
<1.00
<2.95
3.93
5.88
7.83
9.78
11.73
13.68
15.63
17.58
19.53
21.48
23.43
25.38
27.33
29.28
31.23
33.18
35.13
37.08
>38.05
>40.00
B
C
D
E
ccRCC ptPBL
cdPBL
1
0.8
0.6
0.4
0.2
0
-0.2
-0.4
-0.6
-0.8
-1

Supplemental Figure S4: Validation and analysis of pan-cancer and polarizing CD8+ DEGs across new RCC cohort. (**A**) Demonstration of raw Biomark HD generated heatmap providing evidence that all RNA samples and Taqman assays were successful (ladder on right, detection range), (**B-D**) graphical representation of housekeeping genes used for data normalization (*GUSB*, *IPO8*, *PGK*, *POL2RA*, *TBP*) and generation of ΔCT values, where (**B**) are M-values generated by GeNorm for normalization of real-time quantitative RT-PCR data by geometric averaging of multiple internal control genes, and (**C-D**) are SD and Acc. SD (respectively) generated by Norm Finder algorithm for identifying optimal normalization genes. (**E**) Example of correlogram, created using algorithm and -ΔCT normalized values from qRT-PCR validation, and used to find genes across $CD8^+$ cdPBL and $CD8^+$ ccRCC ptPBL validation cohorts that would distinguish possible pan-cancer DEG clusters that would permit efficient stratification of patients according to CD8 ptPBL (Spearman method, coexpression coefficient ladder on right). ccRCC, clear cell renal cell carcinoma; pt, patient; nd, normal donor; PBL, peripheral blood mononuclear cells.

Figure S5

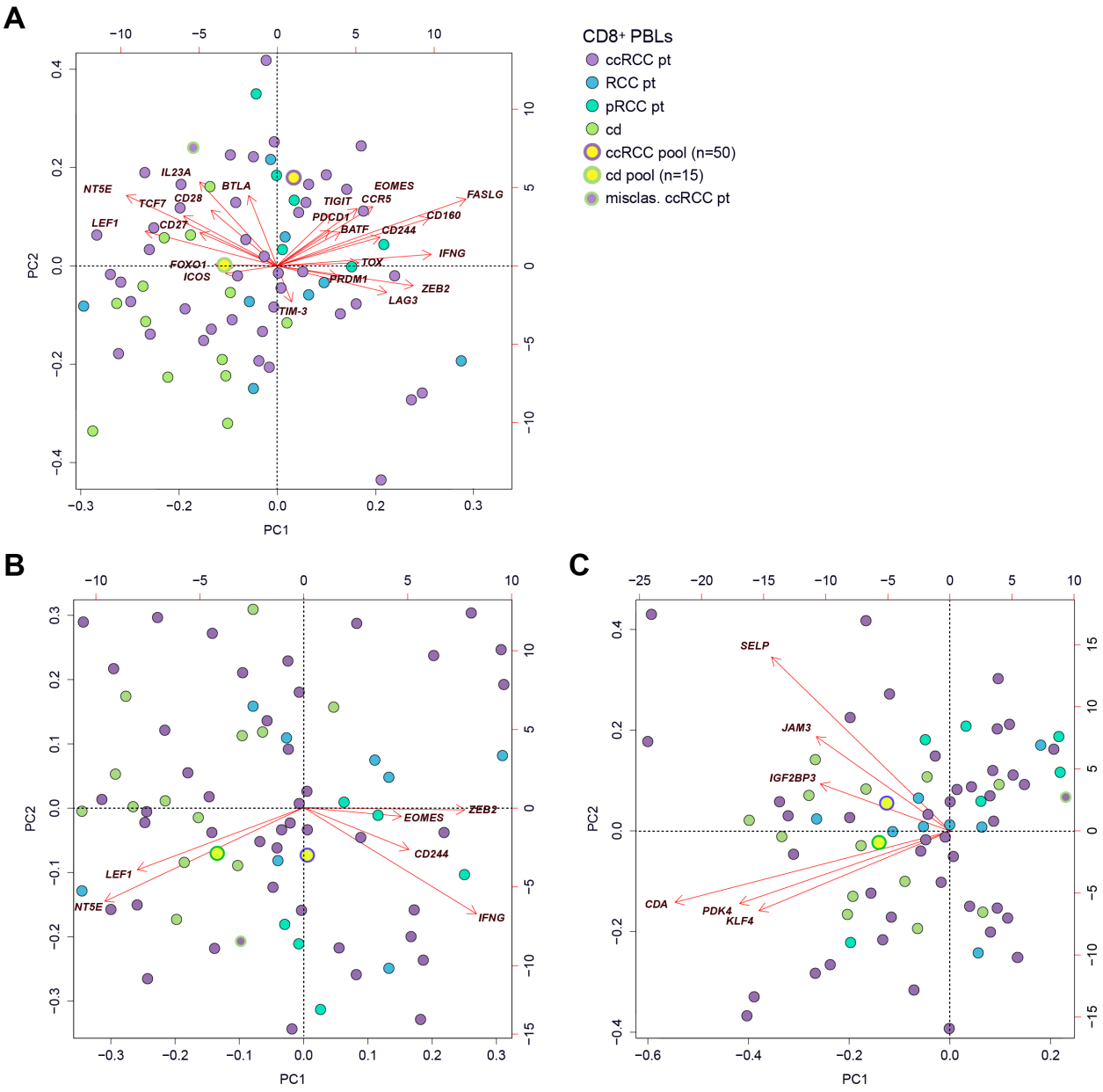
A
B
C
CD8+ PBLs
ccRCC pt
RCC pt
pRCC pt
cd
ccRCC pool (n=50)
cd pool (n=15)
misclas. ccRCC pt
PC1
PC2
IL23A
NT5E
BTLA
CD28
TCF7
LEF1
CD27
FOXO1
ICOS
TIM-3
EOMES
TIGIT
CCR5
PDCD1
BATF
CD244
CD160
FASLG
IFNG
TOX
PRDM1
ZEB2
LAG3
SELP
JAM3
IGF2BP3
CDA
PDK4
KLF4

Supplemental Figure S5: Independent pan-cancer, adhesion, or T cell polarizing gene groups from minimal 32- or 12-gene sets are unable to stratify patients from normal donors. From **Figure 6A**, (**A**) Loss of patient stratification from removal of pan-cancer (*PF4V1*, *CDA*, *PDK4*, *KLF4*, *PIM2*, *TIMP1*, *IGF2BP3*, and adhesion (*JAM3*, *SELP*) DEGs from 32 DEG stratifying signature. From **Figure 6B**, pan-cancer and adhesion markers were analyzed independently from other T cell polarizing DEGs. Normalized -ΔCT qRT-PCR expression values from individual $CD8^+$ T cells isolated from cdPBMC and ptPBMC (PBL) from patients undergoing surgery following RCC diagnosis, were used for principal component analysis (PCA) using applying the euclidean distance metric and complete linkage clustering method (R programming language; R-studio) (*n* = 69). (**B**) Independently assessed top plus bottom PCA DEG groups from **Figure 6B** (*ZEB2*, *EOMES*, *CD244*, *IFNG*, *LEF1*, *NT5E*) are insufficient for stratifying patients from normal donors. (**C**) Independently assessed mid-left PCA DEG group from **Figure 6B** (*CDA*, *PDK4*, *KLF4*, *IGF2BP3*, *JAM3*, *SELP*) are insufficient for stratifying patients from normal donors. ccRCC, clear cell renal cell carcinoma; pRCC, papillary renal cell carcinoma; RCC, renal cell carcinoma; pt, patient; nd, normal donor; misclas., misclassified benign kidney lesion; n, number of patients in pool.

Figure S6

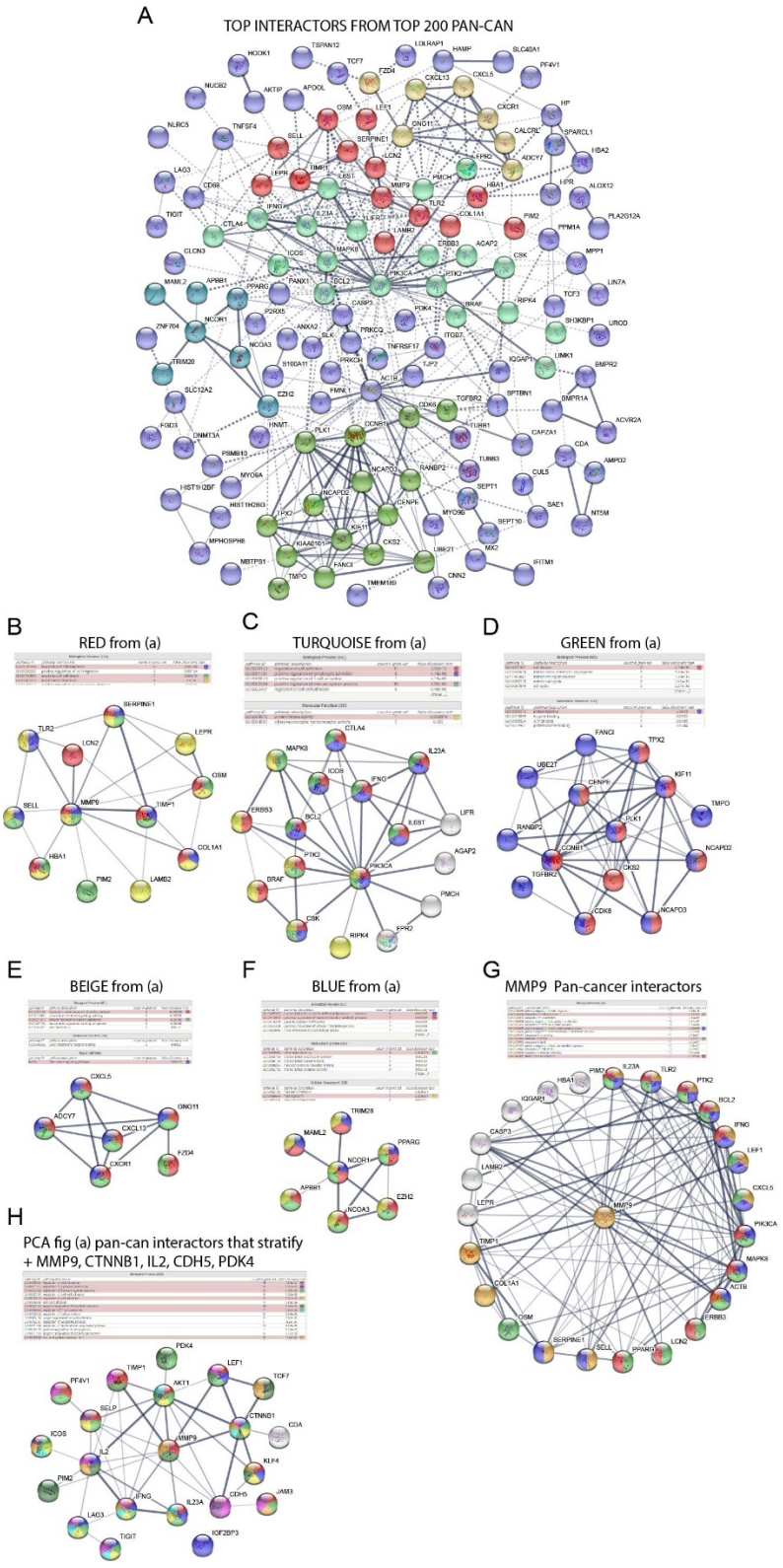
A
TOP INTERACTORS FROM TOP 200 PAN-CAN
B
RED from (a)
C
TURQUOISE from (a)
D
GREEN from (a)
E
BEIGE from (a)
F
BLUE from (a)
G
MMP9 Pan-cancer interactors
H
PCA fig (a) pan-can interactors that stratify
+ MMP9, CTNNB1, IL2, CDH5, PDK4

Supplemental Figure S6. Protein-Protein interaction of top 200 pan-cancer DEGs provide insights on core target pathways and intra pathway linkages. (**A**) Protein-protein interaction (PPI) primary pathways and connecting networks between the top 200 DEGs discovered, with high PPI enrichment value of *P* = 1.85e-10 (String software, v10.5). Unsupervised arrangement and highlighting of distinct pathways in PPI are expanded in **B-G**. (**B**) MMP9, TIMP1 and SERPINE1 are central to regulation of cell death and migration pathways. (**C**) PIK3CA, IFNG, ICOS, BCL2, and CSK are central to cell adhesion and lymphocyte activation pathways. (**D**) CCNB1, PLK1 and CENPE are central to cell division pathway. (**E**) CXCL13, CXCR1, and CXCL5 are central to chemokine signaling pathways. (**F**) NCOR1 is central to positive regulation of transcription cellular pathways. (**G**) MMP9 interacts with more than any other pan-cancer gene, and is a central node of many pathways bridging cell migration and immune system processes (supervised clustering). (**H**) PPI matrix of the pan-cancer DEGs found capable of stratifying patients from normal donors with addition of CTNNB1, IL2, CDH5, and PDK4, involve immune system, cytokine, activation, migration, adhesion and apoptotic cellular pathways.

Figure S7

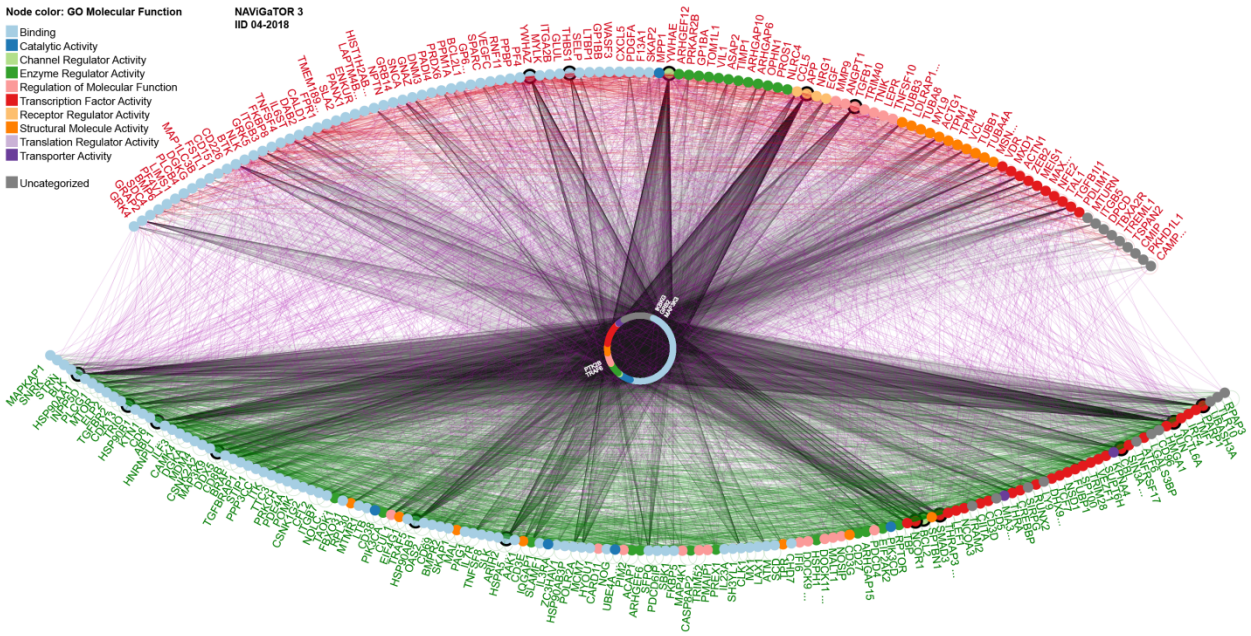

Figure S7. Complete ccRCC ptPBL PPI. Network of all protein-protein interactions (PPIs) among all ccRCC ptPBL DEGs. PPIs obtained from IID ver. 04-2018 and network visualization in NAViGaTOR ver. 3. DEGs increased and decreased in expression and their interacting edges are colored red and green, respectively to demonstrate groupings of these two pan-cancer subclasses, mauve lines highlight interactions between them, and grey lines highlight other protein mediators identified by IID ver. 04-2018. DEG nodes are colored according to GO Molecular Functions described in the legend. Black outline on nodes represents DEGs with the highest number of interacting partners in this network.

Figure S8

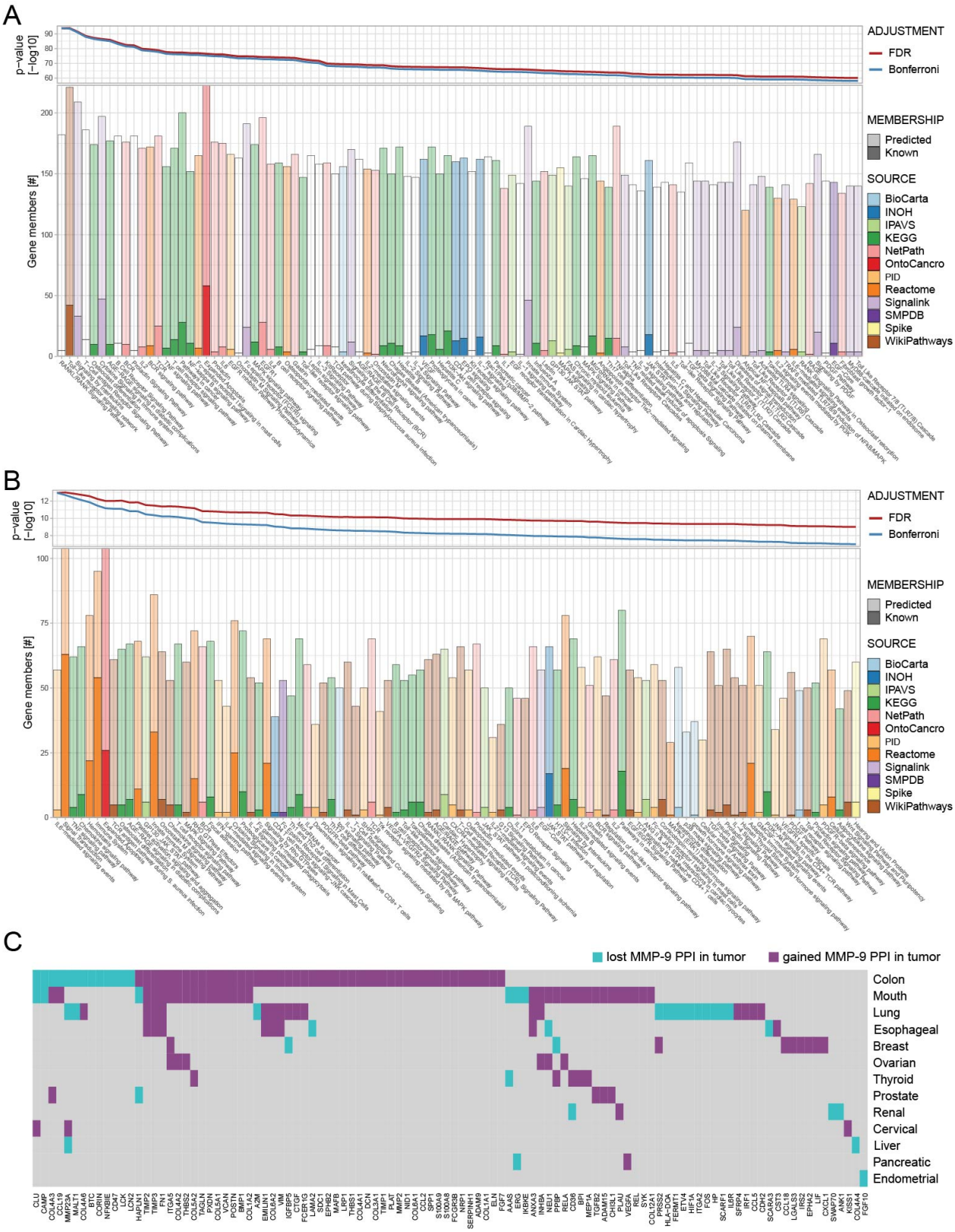
A
p-value [-log10]
ADJUSTMENT
FDR
Bonferroni
MEMBERSHIP
Predicted
Known
SOURCE
BioCarta
INOH
IPAVS
KEGG
NetPath
OntoCancro
PID
Reactome
Signalink
SMPDB
Spike
WikiPathways
Gene members [#]
B
p-value [-log10]
ADJUSTMENT
FDR
Bonferroni
MEMBERSHIP
Predicted
Known
SOURCE
BioCarta
INOH
IPAVS
KEGG
NetPath
OntoCancro
PID
Reactome
Signalink
SMPDB
Spike
WikiPathways
Gene members [#]
C
lost MMP-9 PPI in tumor
gained MMP-9 PPI in tumor
Colon
Mouth
Lung
Esophageal
Breast
Ovarian
Thyroid
Prostate
Renal
Cervical
Liver
Pancreatic
Endometrial

Supplemental Figure S8. MMP-9 extended pathway analyses. (**A-B**) Results of the pathway enrichment analysis as obtained from pathDIP ver. 3 for all ptPBL. MMP-9 pathways associated ptPBL DEGs from pathDIP matrix were correlated, and DEGs which were significantly associated to MMP9 positive pathways ($p<0.05$) were used for pathway scoring and classification. Pathway enrichment analysis graphs depicting results of pathDIP analysis for MMP-9 significant pathway interactors found from correlation analyses. Upper panels shows significance of enrichment obtained for individual pathways expressed as p-value (-log10) adjusted for multiple testing by applying FDR (red) and Bonferroni (blue) methods. Lower barplot shows size of the overlap between query genes and members of individual pathways. Respective numbers of known and predicted pathway members are distinguished by the opacity, and fill color indicates original source of the given pathway. Plots are restricted to top 100 most significantly enriched pathways (full list is found in **Supplemental File S1**). **(C)** Differential gained and lost PPIs of MMP9 in cancers. Gained and lost PPIs of MMP9 in thirteen epithelial tissues-cancers suggesting its tissue-specific role in cancer. MMP9 has 106 disrupted PPIs, 60 of which are specific to only one tissue-cancer. It has the highest number of disrupted PPIs in colorectal, mouth and lung cancers (60, 36, and 29 PPIs, respectively) followed by esophagus with 11 PPIs.

Figure S9

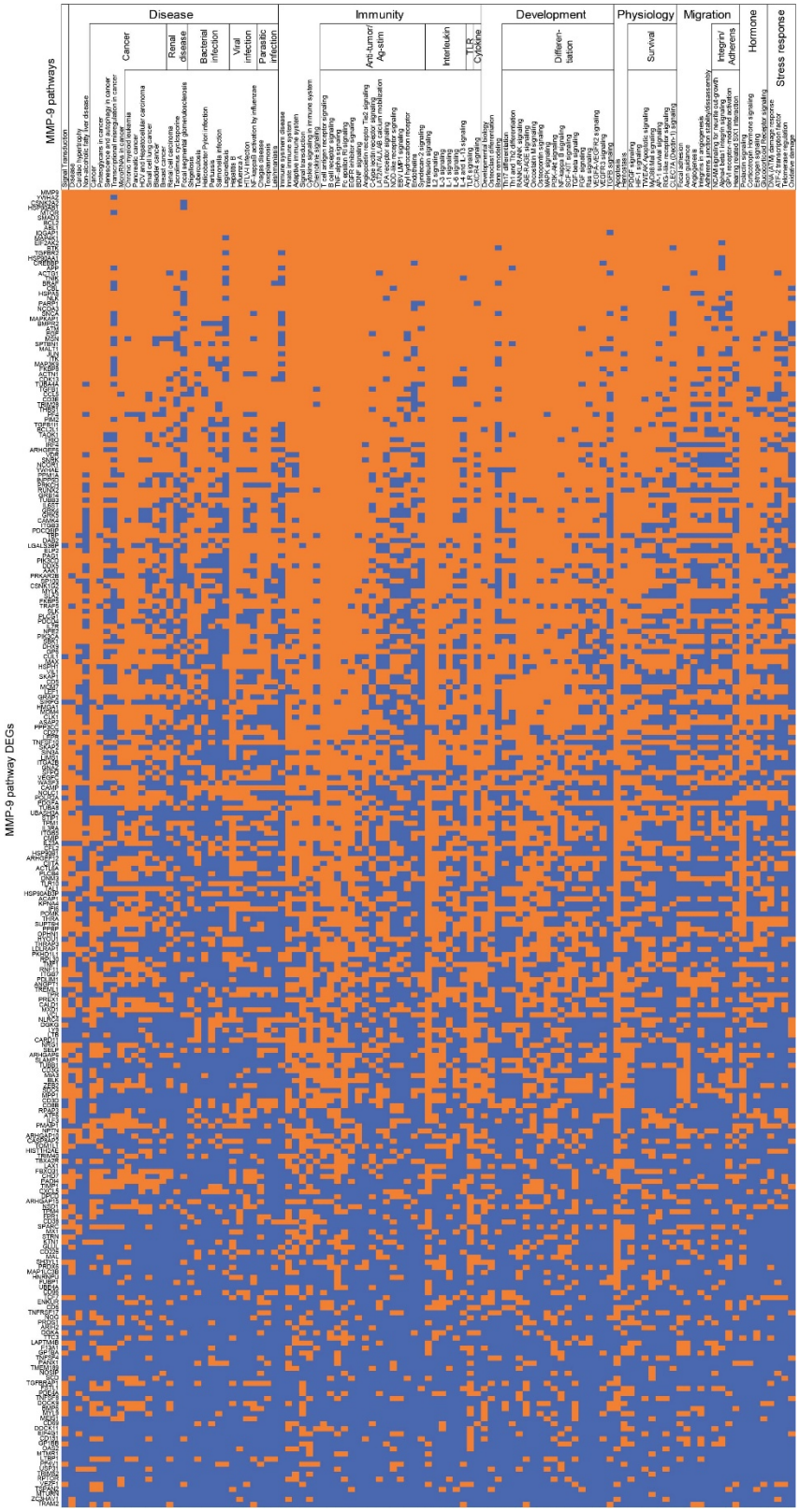
MMP-9 pathways
MMP-9 pathway DEGs
Disease
Immunity
Development
Physiology
Migration
Cancer
Renal disease
Bacterial infection
Viral infection
Parasitic infection
Anti-tumor/ Ag-stim
Interleukin
TLR/ Cytokine
Differen-tiation
Survival
Integrin/ Adherens
Hormone
Stress response

Supplemental Figure S9. MMP9 full pathways DEGs from Figure 7C. Supervised heatmap organizing main correlating MMP-9-pathway genes and associated pathways featuring disease and immunity, followed by differentiation, survival, and migration pathways. Orange, DEG represented in the pathway; blue DEG not represented in the pathway.

Supplemental Tables (see Supplemental materials Supplemental Tables for .xlsx file format)**:**

Table S1

Table S1: Clinicopathological patient parameters.		
No. patients enrolled in study	79	
Surviving patients	76	
tumor size (median, mm)	54.5	
Patient age (median, yrs)	62.5	
Control donor age (median, yrs)	59	
Patient Parameters	*n*	%
Gender		
Male	58	73.4
Female	21	26.6
Histological subtype		
ccRCC	51	64.6
RCC	16	20.2
pRCC	12	15.2
ICD-O Grade ǂ		
1	1	1.3
2	16	20.3
3	45	57.0
4	12	15.2
9	5	6.3
Clinical TNM		
I	43	54.4
II	7	8.9
III	13	16.5
IV	10	12.7
UNKN	6	7.6
TNM-T		
T1	45	57.0
T2	11	13.9
T3	16	20.3
T4	1	1.3
Tx	6	7.6
TNM-N		
N0	70	88.6
N1	5	6.3
Nx	4	5.1
TNM-M		
M0	68	86.1
M1	9	11.4
Mx	2	2.5
Laterality		
left	39	49.4
right	40	50.6
Invasive Tumor Necrosis		
Neg	37	46.8
Pos	31	39.2
UNKN	11	13.9
Family history of cancer		
Yes	15	19.0
No	17	21.5
UNKN	47	59.5

Supplemental Table S1. Clinicopathological patient parameters. Patients and normal donors enrolled in the study. mm, millimeter; yrs, years; *n*, number of patients, %, percentage of total patients; ccRCC, clear cell renal cell carcinoma; pRCC, papillary renal cell carcinoma; RCC, renal cell carcinoma; ICD-O, International Classification of Diseases for Oncology; UNKN, unknown.

Table S2

Table S2: Non-redundant pan-cancer DEGs expressed in T/B cells

Pan-cancer DEG	Evidence in T/B cells (PMID)	Pan-cancer DEG (cont.)	Evidence in T/B cells (PMID) (cont.)
ACTB	22343534	*MMAA*	21943286
ACVR2A	22056434	*MMP9*	28280358
ADCY7	17950003	*MPP1*	21434872
AKTIP (AKT1)	20042722	*MTHFD2*	27325891
ALOX12	24341289; 18046341	*MX2*	27256343
AMPD2	2394745	*MYO9A (myosin IXA)*	24646736
ANKRD22	21347333	*MYO9B*	24646736
ANXA2	8898868	*NCAPD2*	28057211
APBB1 (FE65)	15563829	*NCAPD3*	27737961
ARHGAP18	25207815	*NCOA3*	27111144; 22942430
ARHGAP4	24679343	*NCOR1*	28288100
ARHGEF9 (CDC42)	16439548	*NLRC5*	28615208
ATL1	28240257	*NUCB2*	25880808
BCL2	1924327	*OSM*	8816418
BMPR1A	24350726; 24240189	*P2RX5*	11396717; 25181038
BMPR2	21868697	*P2RY8*	25880808
BRAF	9207797; 21169256	*PACS1*	12855553
CALCRL	22843730	*PANX1*	25301274; 24642372; 20660288; 20884646
CAPZA1	28585036	*PF4V1 (CXCL4L1)*	27828999; 23704819
CASP3	28487480	*PIK3CA (PI3K)*	28685820; 23378844
CCNB1	22950819	*PIM2*	25987564
CD69	19841192	*PLEKHA1*	15626471
CDA	7904595	*PLK1*	22609854
CDC42SE1	25547673	*PMCH*	23775959
CDCP1 (Trask; CDC42)	21559459	*PPARG*	24921943
CDK6	27915416	*PRKCH*	17195206; 25617472
CDKL5	17589290	*PRKCQ*	28152304; 26390157
CENPE (KIF10)	23980113	*PSMB10 (MECL1)*	18025207
CETP	15228446	*PTK2 (FAK)*	24816556
CLEC4D (CLECSF8)	23606632	*PTPRCAP*	9880514
CNN2	23499442; 26046660	*RANBP2 (Nup358)*	19922867
CRYAB	23736536	*RIPK4*	26522402
CSK	28522807	*RORA*	22561605
CTLA4	10101680	*S100A11*	16351635
CUL5	27307564 ; 17449237	*SAA2*	25847238
CXCL13	19095563	*SAE1*	25143484
CXCL5	28003642; 25130611	*SELL*	19654311
CXCR1	12707326	*SEPT1*	19043408
DGKE	18689679	*SEPT10*	18077723
DNMT3A	27582468; 27690235	*SH3KBP1 (CIN85)*	21708930
DOCK9	23396170; 19898472	*SH3YL1*	22927640
ERBB3	20668683	*SIGLEC1*	22192781
EZH2	28490575	*SIGLEC12*	27548433
FGD6	18838382	*SIPA1L1*	12958214; 17702895
FMNL1	23874337	*SLC12A2*	27400149
FNBP4	27835906	*SLK*	19255442
FPR2 (ALX)	24166736	*SNRK*	27936095; 18927432
FZD4	21549744	*SORL1*	26487345
GAS2L3	23469016	*SPARCL1*	27085068
GNG11	15914563; 20670477	*SPTBN1*	15965501; 12354383; 21877118
HAMP	23647063	*TBC1D10C (EPI64C)*	18450757; 27021007
HBA1 (CD31)	14701691; 23761922	*TCF3*	25990863; 23396170
HIST1H2BF	27213115	*TCF7*	27111144
HIST1H2BG	27371726	*TCIRG1 (TIRC7)*	15294947
HOOK1	12791665	*TGFBR2*	24098055;25677619; 28472799
HP (haptoglobin)	10664448; 12562322	*THSD7A*	28669992
HPR	9673399	*TIGIT*	19011627
ICOS	11343121	*TIMP1*	18502033
IFITM1 (Leu-13)	9597125	*TLR2*	27622036
IFNG	25480562	*TMEFF1 (tomoregulin-1)*	25380171; 18523280; 12618130
IGF2BP3	27881740	*TMEM189*	27371726
IL23A	16688182	*TMPO*	9199966
IL6ST	20951741	*TNFAIP2*	21921781
IQGAP1	22573807	*TNFRSF17*	29504446
ITGB7	20926792	*TNFSF4 (OX40-L)*	10586044; 8076595
KIF11	27875993	*TPX2*	27910998; 14701852
LAG3	25780040	*TRAF1*	22570473
LCN2	26671823; 25010215	*TREML1*	16670310
LDLRAP1	21918187	*TRIM28*	23169648; 22544392
LEF1	27111144	*TRPM2*	26300888
LIFR	25514345	*TSPAN12*	20159112
LIMK1	11784854	*TUBB1*	19583510
LPPR2	21939632	*TUBB3*	26028645; 20220512
MAML2	17699740	*UNC119B*	14757743
MAPK8 (JNK)	14563325	*ZNF385A*	22945289
MAST4	18650832	*ZNF704*	24086395
MBTPS1 (S1P)	21402360		

Supplemental Table S2. Non-redundant pan-cancer DEGs expressed in T/B cells. Pan-cancer DEGs discovered from ccRCC ptPBL and TIL from profiling TCGA, GEO and EGA, ccRCC, NSCLC, BC, GI and OV cancers datasets using KM plotter. From a Total of 467 DEGs discovered (see **Supplemental Figure S1**), those that have been cited in the literature as being expressed by T or B cells are shown here, with redundancies of DEGs discovered as expressed in both isolates merged for simplicity of table presentation. Common names are shown in brackets in some instances. PMID, Pubmed ID.

Table S3

Table S3: Top 100 Pan-cancer DEGs with scoring and literature

ptPBL DEG	pan-cancer score (%)	correlation score (%)	Gene name	ptPBL PMID	TIL DEG	pan-cancer score (%)	Gene name	TIL PMID
TREML1	41	0	Triggering receptor exp	16670310	*PMCH*	56	Pro-melanin-concentr	23775959
PF4V1	61	29	CXCL4L1/C-X-C motif	23704819	*IFNG*	46	Interferon gamma	25480562
HBA1	41	0	CD31/Hemoglobin, alp	23761922	***LAG3***	61	Lymphocyte-activatio	25780040
IL23A	61	29	Interleukin-23 subunit a	16688182	*TMPO*	54	Thymopoietin	9199966
MPP1	51	29	Membrane protein, palt	21434872	*TBC1D10C*	21	TBC1 domain family,	18450757; 2
MMP9	71	43	Matrix metalloproteinas	28280358	***CCNB1***	80	Cyclin B1	22950819
GNG11	46	86	G protein gamma 11	15914563; 206	*CENPE*	66	Centromere-associat	23980113
ARHGAP18	46	0	Rho GTPase activating	25207815	***PIM2***	71	Pim-2 oncogene	25987564
PDK4	46	71	Pyruvate dehydrogenas	n/a	***NCAPD2***	100	CAP-D2/Non-SMC c	28057211
FPR2	61	29	Formyl peptide recepto	24166736	***PTPRCAP***	61	CD45-associated pro	9880514
LCN2	51	14	Lipocalin-2	25010215	*EZH2*	73	Enhancer of zeste ho	28490575
HIST1H2BG	83	29	Histone cluster 1, H2bg	27371726	*LIMK1*	76	LIM domain kinase 1	11784854
TIMP1	80	14	Tissue inhibitor of meta	18502033	*TIGIT*	61	T cell immunorecepto	19011627
PPM1A	24	100	Protein phosphatase 1	n/a	***CASP3***	61	Caspase 3	28487480
TMEFF1	80	14	Tomoregulin-1	18523280; 126	*TPX2*	86	TPX2, microtubule-as	27910998; 1
IGF2BP3	66	43	Iinsulin-like growth facto	27881740	***TRPM2***	80	Transient receptor po	26300888
PANX1	54	0	Pannexin-1	25301274; 246	***CSK***	90	C-src tyrosine kinase	28522807
LDLRAP1	34	57	Low density lipoprotein	21918187	*PSMB10*	54	Proteasome subunit b	18025207
CDA	80	0	Cytidine deaminase	7904595	***TNFAIP2***	80	Tumor necrosis factor	21921781
IL6ST	66	0	CD130/interleukin 6 sig	20951741	*IFITM1*	61	Interferon induced tra	9597125
CETP	51	14	Cholesteryl ester transf	15228446	*MX2*	56	Interferon-induced GT	27256343
MYO9B	41	0	Myosin-Ixb	24646736	*TCIRG1*	54	T-cell immune regulat	15294947
DGKE	56	0	Diacylglycerol kinase e	18689679	*NCAPD3*	66	Non-SMC condensin	27737961
MPHOSPH8	76	86	M-phase phosphoprote	n/a	*PLK1*	76	Polo-like kinase 1	22609854
PRKCH	44	0	Protein kinase C, eta	17195206; 256	***ACTB***	61	Actin, beta	22343534
ADCY7	44	14	Adenylate cyclase 7	17950003	*GAS2L3*	86	Growth arrest-specific	23469016
IQGAP1	66	57	IQ motif containing GTF	22573807	***ARHGAP4***	61	Rho GTPase activatir	24679343
FMNL1	51	14	Leukocyte formin	23874337	*HAMP*	66	Hepcidin	23647063
NCOA3	34	0	Nuclear receptor coacti	27111144; 229	***MTHFD2***	80	Methylenetetrahydrof	27325891
TNFRSF17	57	14	B-cell maturation protei	26370838; 245	***KIF11***	80	Kinesin family membe	27875993
TCF3	57	86	Transcription factor 3	23396170	*MAST4*	63	Microtubule-associat	18650832
NCOR1	66	0	Nuclear receptor co-rep	28288100	*APBB1*	46	Amyloid beta A4 prot	15563829
BCL11B (ATL1)	46	71	Alkyltransferase-like pr	28240257	*UNC119B*	63	Protein unc-119 hom	14757743
ITGB7	63	29	Integrin beta-7	20926792	*MMAA*	66	Methylmalonic aciduri	21943286
RANBP2	66	14	RAN binding protein 2	19922867	*PTK2*	46	Focal adhesion kinas	24816556
SNRK	66	43	SNF related kinase	27936095; 189	*PPARG*	63	Peroxisome proliferat	24921943
TGFBR2	70	71	Transforming growth fa	24098055; 256	*BMPR1A*	66	Bone morphogenetic	24350726; 2
SLK	76	71	STE20-like kinase	19255442	*SEPT10*	76	Septin 10	18077723
FNBP4	34	100	Formin binding protein	27835906	*CUL5*	63	Cullin-5	27307564; 1
NUCB2	46	29	Nucleobindin 2	25880808	*MAPK8*	76	Mitogen-activated pro	14563325
BRAF	66	0	Serine/threonine-protei	9207797; 2116	*ACVR2A*	46	Activin receptor type-2	22056434
UBE2T	61	14	Cell proliferation-induci	n/a	*PPAP2A*	76	Phosphatidic acid ph	21576386
CD69	47	0	Early T-cell activation in	19841192	*LIFR*	66	Leukemia inhibitory fa	25514345
DOCK9	54	86	Dedicator of cytokinesi	23396170; 198	*RORA*	56	RAR-related orphan r	22561605
SPTBN1	86	0	Spectrin, non-erythroid	15965501; 123	*TSPAN12*	66	Tetraspanin 12	20159112
PIK3CA	46	71	PI3K/phosphoinositide-	28685820; 233	*PLEKHA1*	56	Pleckstrin homology d	15626471
SH3YL1	46	14	SH3 domain-containing	22927640	*SIPA1L1*	66	Signal-induced prolife	12958214; 1
SORL1	56	14	Sortilin-related recepto	26487345	*AKTIP*	46	AKT interacting prote	20042722
LEF1	41	0	Lymphoid enhancer-bir	27111144	*ZNF704*	46	Zinc finger protein 70	24086395
SLC12A2	56	0	Solute carrier family 12	27400149	*FZD4*	56	Frizzled homolog 4	21549744

Supplemental Table S3. Top 100 Pan-cancer DEGs with scoring and literature.
Top 100 Pan-cancer DEGs selected from 4-pronged scoring system (see Supplemental fig. S1). Red highlighted DEGs are increased in expression, whereas green highlighted DEGs are decreased in expression in training set ccRCC. Dark red or green highlighted DEGs are interactors (e.g., Figure 3). Underlined are common to both PBCM and TIL. Bold DEG gene names are only expressed in lymphoid/myeloid tissues and are modified in expression across 17 cancers (The Protein Atlas). Pan-cancer scores from increased or decreased in tumor relative to normal tissues, and positive or negative effect on overall survival (scores >50% are highlighted). Correlation scores are calculated from ccRCC microarrays (scores >0% are highlighted according to degree). Gene names added in instances where PMID uses this notation. PMID, Pubmed ID. ptPBL listed DEGs are genes discovered from ccRCC training microarray dataset where DEG was higher in ptPBL than cdPBL. TIL listed DEGs are genes discovered from ccRCC training microarray dataset where DEG was higher in TIL than TIIC (-1.5 to 1.5 Fold-change cut-off; FDR P = 0.05).

Table S4

Table S4: Selected Pan-cancer and T cell polarizing DEGs for validation

Gene	Gene Name	UNIPRO	Aliases	Assay ID	Lymp	Oth	Function classific	Functions	Pan-can fun	PMID	Pan-car	PMCID
BATF	Basic leucine zipper tra	Q16520	BATF1, SFA2	Hs00232390_m1	CD4, CD8		Transcription factor	Transcription factor, negative regulator of			B-cell-activating trans	
BCL11B	B-cell CLL/lymphoma 1	Q9C0K0	ATL1, CTIP2, RIT1	Rh02853704_m1	CD8		Transcription factor	Transcription factor, T-cell differentiation, neg			regulation of apop	
BCL6	B-cell CLL/lymphoma 6	P41182	LAZ3	Hs00153368_m1	CD4, CD	B	Transcription factor	Transcription factor, transcription of STAT			Tfh master regulator	
BCOR	BCL6 corepressor	Q6W2J9	ANOP2, MAA2, MCO	Hs00372378_m1	CD8		Transcription factor	Corepressor of BCL6				
BTLA	B and T lymphocyte as	Q7Z6A9	CD272, BTLA1	Hs00699198_m1	CD4, CD	B	Inhibitory TCR corece	Inhibitory signal				
CCR4	C-C motif chemokine re	P51679	CD194, CKR4, CMKB	Hs00356611_s1	CD4	mφ	Cytokine/chemokine r	Receptor for MIP-1, RANTES, TARC and			Th17, Th22	
CCR5	C-C motif chemokine re	P51681	CD195, CKR5, CMKB	Hs99999149_s1	CD4, CD	B, DC	Cytokine/chemokine r	Receptor for MCP-2, MIP-1α, MIP-1β and			RANTES	
CCR6	C-C motif chemokine re	P51684	CD196, CKRL3, CMKI	Hs01890706_s1	CD4, CD	B, DC	Cytokine/chemokine r	Receptor for MIP-3α			Th17, Th22	
CD160	CD160 molecule	O95971	BY55, NK1, NK28	Hs00199894_m1	CD8	NK	Inhibitory TCR corece	Tightly associated with peripheral blood NI			Generation and maint	
CD244	CD244 molecule	Q9BZW8	2B4, NKR2B4, SLAMF	Hs00175568_m1	CD4, CD	NK, m	Inhibitory TCR corece	Activation, cytokine production, adhesion a			inhibitory role on M. t	
CD27	CD27 molecule	P26842	TNFRSF7	Hs00386811_m1	CD4, CD	B, NK,	Surface protein	Costimulation signal				
CD28	CD28 molecule	P10747	TP44	Hs01007422_m1	CD4, CD	plasm	Activating TCR corece	Costimulation and proliferation of T cells following CD80/86 enga				
CD6	CD6 molecule	P30203	TP120	Hs00198752_m1	CD4, CD	B	Surface protein	Adhesion, T-cell and APC interactions				
CD69	CD69 molecule	Q07108	AIM, BL-AC/P26, CLE	Hs00934033_m1	CD4, CD	B, NK,	Activating TCR corece	Activation, cytokine production, NK-mediated lysis				
CDA	cytidine deaminase	P32320	CDD	Hs00156401_m1			Metabolism	CDA expressior	27601591		CDA and A	2727621
CTLA4	cytotoxic T-lymphocyte	P16410	ALPS5, CD, CD152, C	Hs03044418_m1	CD4, CD	B	Inhibitory TCR corece	Inhibitory signal to T cells				
CXCL13	C-X-C motif chemokine	O43927	ANGIE, ANGIE2, BCA	Hs00757930_m1	CD8		Cytokine/chemokine r	B-cell chemotaxis, homing to follicules			expressed by Tfh, B l	
CXCR3	C-X-C motif chemokine	P49682	CD182, CD183, CKR-	Hs01847760_s1	CD4, CD	NK, m	Cytokine/chemokine r	Receptor for IL-8			Th1	
CXCR5	C-X-C motif chemokine	P32302	CD185, BLR1, MDR1	Hs00540548_s1			Cytokine/chemokine r	Receptor for BLC, B-cell migration			Tfh	
DGKA	diacylglycerol kinase al	P23743	DAGK, DAGK1	Hs01548908_g1	CD4, CD8		Metabolism	Signaling molecule				
DGKE	diacylglycerol kinase e	P52429	AHUS7, DAGK5, DAG	Hs00177537_m1			Signaling	regulate TCR s	1.9E+07		this may b	5065962
DGKZ	diacylglycerol kinase ze	Q13574	DAGK5, DAGK6, DG	Hs01632414_s1	CD4, CD8		Signaling	Negative regulation of Ras signaling, migration, mitotic G1 DNA c				
EOMES	eomesodermin	O95936	TBR2	Hs00172872_m1	CD4		Transcription factor	Transcription factor, adaptive immunity, T-			Associated with termi	
ETS1	ETS proto-oncogene 1,	P14921	P54, ETS-1, EWSR2	Hs00428293_m1	CD4, CD8		Transcription factor	differentiation, Transcription factor, angiog			promote Th1 and inhib	
FASLG	Fas ligand	P48023	ALPS1B, APT1LG1, A	Hs00181225_m1	CD4, CD	NK, ne	Apoptosis	Apoptosis triggered by binding to FAS			Cytolytic CD4 T cells	
FOXO1	forkhead box O1	Q12778	FKH1, FKHR, FOXO1	Hs01054576_m1	CD4, CD8		Transcription factor	Transcription factor, apoptosis, autophagy,			cell differentiation, gl	
FOXP3	forkhead box P3	Q9BZS1	AIID, DIETER, IPEX,	Hs01085834_m1	CD4		Transcription factor	Transcriptional regulator, B-cell homeosta			Treg master regulato	
GATA3	Gene Symbol:GATA3	P23771	HDR	Hs00231122_m1	CD4, CD8		Transcription factor	Transcription factor, coagulation, Wnt signaling, cellular response				
GUSB	glucuronidase beta	P08236	BG, MPS7	Hs99999908_m1	CD4, CD8		Housekeeping	Lysosomal enzyme			Housekeeping gene	
HAVCR2	hepatitis A virus cellular	Q8TDQ0	CD366, TIM-3	Hs00262170_m1	CD4, CD8, Th1		Inhibitory TCR corece	Activation of mφ, tolerance, inhibition of au			TIM-3 is Expressed o	
HIST1H2BG	histone cluster 1, H2bg	P62807	H2BFA	Hs00374317_s1			Activation	T cell activation	23624600		activated T	1865317
ICOS	inducible T-cell costimu	Q9Y6W8	CD278, AILIM, CVID1	Hs00359999_m1	CD4, CD8, Th2		Activating TCR corece	Activation and proliferation of T cells			Generation and maint	
IFNG	interferon gamma	P01579	IFNγ	Hs00989291_m1	CD4, CD	DC, NI	Cytokine/chemokine r	Pro-inflammatory cytokine				
IGF2BP3	insulin like growth facto	O00425	CT98, IMP3, KOC, KC	Hs00559907_g1			Translational regulation	IGF2BP3 targe	2.7E+07		Enforced e	4811152
IKZF1	IKAROS family zinc fin	Q13422	IKAROS, LYF1	Hs00958474_m1	CD4, CD8		Transcription factor	Transcription factor, lymphocyte develop			Chromatin remodeling	
IKZF3	IKAROS family zinc fin	Q9UKT9	AIOLOS	Hs00232635_m1	CD4, CD8		Transcription factor	Transcription factor, lymphocyte development				
IKZF4	IKAROS family zinc fin	Q9H2S9	EOS	Hs00223842_m1	CD4		Transcription factor	Transcription factor, lymphocyte develop			Critical mediator of FO	
IL10	interleukin 10	P22301	TGIF, IL10A, CSIF, C	Hs00961622_m1	CD4	mono	Signaling	Down-regulates expression of Th1 cytokin			Treg	
IL17A	interleukin 17A	Q16552	IL-17, CTLA-8	Hs00174383_m1	CD4, CD8		Signaling	Pro-inflammatory cytokine, Th17				
IL18RAP	interleukin 18 receptor	O95256	ACPL, CD218B, IL-18	Hs00977695_m1	CD4		Signaling	Pro-inflammatory cytokine, cell-mediated immunity				
IL22	interleukin 22	Q9GZX6	TIFA	Hs01574154_m1	CD4, CD	DC	Signaling	Pro-inflammatory cytokine, initiation of innate immune responses				
IL23A	interleukin 23 subunit al	Q9NPF7	IL23, P19, SGRF	Hs00372324_m1			Signaling	IL-23 is an impc	1.7E+07		IL-23 is as	3701076
IL6ST	interleukin 6 signal tran	P40189	CD130, GP130, IL6RE	Hs00174360_m1			Signaling	B cell lymphom	20951741;		20042455;	2203840
IL7R	interleukin 7 receptor	P16871	CD127, IL7RA	Hs00902334_m1	CD4, CD	B	Signaling	Receptor of IL-7				
IPO8	importin 8	O15397	RANBP8	Hs00183533_m1	CD4, CD8		Housekeeping	Nuclear import			Housekeeping gene	
IQGAP1	IQ motif containing GTI	P46940	HUMORFA01, SAR1,	Hs00896595_m1			Inhibitory TCR corece	ptor	IQGAP1 regula	22573807	IQGAP1: I	4480615
IRF1	interferon regulatory fa	P10914	MAR	Hs00971960_m1	CD8		Transcription factor	Activator of IFN-α and IFN-β production				
IRF4	interferon regulatory fa	Q15306	MUM1, LSIRF, NF-EM	Hs01056533_m1	CD8		Transcription factor	Activator of IFN production			Th9 master regulator?	
JAK1	Janus kinase 1	P23458	JTK3	Hs01026983_m1	CD4		Signaling	Signaling molecule for IFN				
JAM3	junctional adhesion mol	Q9BX67	JAM-2, JAM-3, JAM-C	Hs00230289_m1			Adhesion	T lymphocyte, NK cell, and dendritic cell traffick				
JUN	Jun proto-oncogene, Al	P05412	AP-1, C-JUN	Hs01103582_s1	CD4		Transcription factor	Regulates gene expression				
KLF4	Kruppel like factor 4	O43474	EZF, GKLF	Hs00358836_m1	CD8		Transcription factor	Transcription factor, controls G1-to-S transition when DNA damn				
LAG3	lymphocyte activating 3	P18627	CD223	Hs00158563_m1	CD4, CD	NK	Inhibitory TCR corece	Activation of immune responses			LAG-3 expression def	
LEF1	lymphoid enhancer-binc	Q9UJU2	TCF1A	Rh01553173_m1	CD8		Transcription factor	Transcription factor, enhancer of TCR activity, involved in Wnt pa				
MKI67	marker of proliferation	P46013	KI-67, KIA, MIB-1, PP	Hs01032443_m1	CD4		Proliferation / Chroma	Nuclear protein, proliferation			KI-67	
MMP9	matrix metallopeptidase	P14780	CLG4B, GELB, MANC	Hs00957562_m1			Activation	MMP9, may fur	2063945		Regulate A	3095987;
MPHOSPH8	M-phase phosphoprote	Q99549	HSMPP8, TWA3, MPF	Hs00736882_m1			Transcription factor	MPP8 targets t	20871592		Knockdow	5482300
NCAPD2	non-SMC condensin I c	Q15021	CAP-D2, CNAP1, Cap	Hs00274505_m1			Chromosome condensation	A mutation in a	Kleisin-be		Condensin	Associated
NFIL3	nuclear factor, interleuk	Q16649	E4BP4, IL3BP1, NFIL3	Hs00705412_s1	CD8		Transcription factor	Transcription factor, represses PER1 and 2				
NOC2L	NOC2 like nucleolar as	Q9Y3T9	NET15, NET7, NIR, PI	Hs04194444_g1	CD8		Transcription factor	HDAC-independant inhibitor of HAT				
NT5E	5'-nucleotidase ecto	P21589	CALJA, CD73	Hs00159686_m1	CD4, CD8		Inhibitory TCR corece	Conversion of extracellular nucleotides to membrane-permeable				
PDCD1	programmed cell death	Q15116	PD-1	Rh03418231_m1	CD8		Inhibitory TCR corece	T-cell function, inhibitory signal				
PDK4	pyruvate dehydrogenas	Q16654	none	Hs01037712_m1			Metabolism	the negative re	1.8E+07			
PF4V1	platelet factor 4 variant	P10720	CXCL4L1, PF4A, SCY	Hs01891271_s1			Cytokine/chemokine	CXCL4L1 Inhibi	17575164		Platelet fa	3904624;
PGK	phosphoglycerate kinas	P00558	MIG10, PGKA	Hs99999906_m1	CD4, CD8		Housekeeping	Cofactor for polymerase α, angiogenesis			Housekeeping gene	
PIM2	Pim-2 proto-oncogene,	Q9P1W9	none	Hs00179139_m1			Proliferation	Pim-2 Kinase Ir	25987564		In Socs3-Stat1, 3&5 r	
POLR2A	RNA polymerase II sub	P24928	POLR2, POLRA, RPB	Hs00172187_m1	CD4, CD	All	Housekeeping	Largest subunit of polymerase II, synthesi			Housekeeping gene	
PRDM1	PR domain 1	O75626	BLIMP1	Hs00153357_m1	CD8		Transcription factor	Repressor of IFN-β			Th2 cells by repressin	
RORA	RAR related orphan re	P35398	NR1F1, ROR1, ROR2	Hs00536545_m1	CD4, CD8		Transcription factor	Nuclear hormone receptor, transcription factor, enhancer of gene				
RORC	RAR related orphan re	P51449	IMD42, NR1F3, RORC	Hs01076122_m1	CD4		Transcription factor	Transcription factor, key molecule in differ			Th17 master regulato	
RPL13A	ribosomal protein L13a	P40429	L13A, TSTA1	Hs04194366_g1			Housekeeping				Housekeeping gene	
RUNX1	runt related transcriptio	Q01196	AML1, CBFA2, EVI-1,	Hs01021971_m1	CD4, CD8		Transcription factor	Transcription factor, insures normal hemat			Th1 regulator, inhibitor	
RUNX3	runt related transcriptio	Q13761	AML2, CBFA3, PEBP2	Hs00231709_m1	CD4		Transcription factor	Transcription factor, tumor suppressor				
SELP	selectin P	P16109	CD62, CD62P, GMP1	Hs00927900_m1			Adhesion	essential role in the initial recruitment of leukocy				
SLAMF1	signaling lymphocytic a	Q13291	IPO-3, CD150, SLAM	Hs00234149_m1	CD4, CD	B, DC	Activating	Stimulation and activation of cells			expressed on γδ T cel	
SLK	STE20 like kinase	Q9H2G2	LOSK, STK2	Hs00207000_m1			Signaling	Germinal cente	27465533		Germinal c	4002213;
SMAD3	SMAD family member 3	P84022	MADH3, HSPC193, JV	Hs00969210_m1			Transcription factor	Signal transducer, transcriptional modulat			Smad3 binding to the	
SNRK	SNF related kinase	Q9NRH2	HSNFRK	Hs00299395_m1			Metabolism	mutations in du	27936095		Snrk-1 ove	3475258
SPI1	Spi-1 proto-oncogene	P17947	OF, PU.1, SFPI1, SPI	Hs02786711_m1	CD4		Transcription factor	Transcription factor, myeloid and B-lymph			Th9 master regulator?	
SPRY2	sprouty RTK signaling a	O43597	IGAN3	Hs01921749_s1	CD4		Inhibitory	Inhibition of RTK signaling				
SPTBN1	spectrin beta, non-eryth	Q01082	ELF, HEL102, SPTB2	Hs00162271_m1			Transcription factor	Called Spectrin	25096061		spectrin-ar	2857017
STAT3	signal transducer and a	P40763	ADMIO, ADMIO1, API	Hs00374280_m1	CD4		Transcription factor	Transcription activator following stimulation by IFN-α, IFN-γ, IL-5				
STAT4	signal transducer and a	Q14765	SLEB11	Hs01028017_m1	CD4		Transcription factor	Transcription activator essential to IL-12 r			Th1 regulator, induced	
STAT6	signal transducer and a	P42226	D12S1644, IL-4-STAT	Hs00598625_m1	CD4		Transcription factor	Transcription activator essential to IL-4 re			Th2 regulator	
TBP	TATA-box binding prote	P20226	TFIID, GTF2D, GTF2	Hs99999910_m1	CD4, CD8		Housekeeping	Coordination of initiation of transcription by			Housekeeping gene	
TCF7	transcription factor 7 (T	P36402	TCF-1	Hs00175273_m1	CD8		Transcription factor	Transcriptional activator, differentiation				
TGFBR2	transforming growth fa	P37173	AAT3, FAA3, LDS1B,	Hs00234253_m1			Signaling	Guardian of T C	24098055;			
TIGIT	T-cell immunoreceptor	Q495A1	VSIG9, VSTM3, WUC	Hs00545087_m1	CD4, CD8, Tfh		Inhibitory TCR corece	Regulates T-cell dependant B-cell responses				
TIMP1	TIMP metallopeptidase	P01033	CLGI, EPA, EPO, HCI	Hs01092512_g1			Protein regulation	Regulates MMF	1850203		TIMP1 anc	5305237;
TMEFF1	transmembrane protein	Q8IYR6	H7365, TR-1	Hs00186495_m1			Migration	crucial inhibitor of the Noc	TMEFF1) i			280611;
TNF	tumor necrosis factor	P01375	DIF, TNF-alpha, TNFA	Hs01113624_g1	CD4	mφ	Transcription factor	Pro-inflammatory cytokine, proliferation, differentiation and apopt				
TNFRSF4	TNF receptor superfam	P43489	OX40, CD134, ACT35	Hs00937194_g1			Transcription factor re	TNF-receptor, T-cell activation and apoptosis, induces expressio				
TNFRSF9	TNF receptor superfam	Q07011	4-1BB, CD137, ILA	Hs00155512_m1	CD4, CD	B, mor	Transcription factor re	Clonal expansion, survival, and development of T cells				
TOX	thymocyte selection as	O94900	TOX1	Hs01055573_m1	CD8		Transcription factor	Involved in chromatin assembly, transcription and replication, T-c				
TRAF5	TNF receptor associate	O00463	MGC:39780, RNF84	Hs00182979_m1	CD4		Cytokine/chemokine	Transducer of TNF signal				
ZEB2	zinc finger E-box bindin	O60315	SIP-1, SMADIP1	Hs00207691_m1	CD4		Transcription factor	Transcriptional repressor activated by SMADs				

Supplemental Table S4. Selected Pan-cancer and T cell polarizing DEGs for validation. DEGs selected for validation on new RCC cohort ptPBL $CD8^+$ T cells. Assay IDs represent TaqMan assays codes used. Pan-cancer DEGs are in bold. PMID (Pubmed ID) and PMCID (Pubmed central ID) and notes are reference for pan-cancer functions and link to immunity.

Table S5

Table S5: Comparison of DEGs validation assays to HIV-1 elite controllers.

			RCC ptPBL / cdPBL			HIV-1 Elite	PMID	
		DEG	Avg.LogFC	P value	t ratio	Avg.LogFC	Cancer	HIV-1
DEG impact on HIV-1 replication and cancer progression	non-permissive	TIMP1	7.897	0.0868	1.744	0.004	26258010	25136083
		FOXO1	4.217	<0.0001	5.495	0.302	18391973	25330112
		CD69	1.434	0.0928	1.757	0.176	23954168	28053103
		IL7R	1.305	0.0001	4.723	0.598	28314253	22693657
		IL23A	1.259	0.0116	2.611	0.109	25008775	29091911
		IRF1	1.154	0.0423	2.079	0.119	23807161	17502719
		RUNX3	1.135	0.0043	2.952	0.100	25008775	24651404
		IKZF1	1.080	0.0115	2.757	0.189	28471446	21933919
		STAT4	1.070	0.0003	3.778	0.191	21998209	29212666
	permissive	4-1BB	0.846	0.0934	1.707	-0.370	22232735	19406689
		SPI1	0.796	0.0614	1.910	-0.056	28415748	24503097
		PIM2	0.782	0.0009	3.503	-0.018	27901106	25207815
		STAT6	0.763	0.0253	2.299	-0.126	21595984	11371617
		LAG3	0.735	0.0078	2.760	-0.637	28258692	25738606
		CDA	0.711	0.0120	2.630	-0.035	27601591	15713780
		FASLG	0.482	<0.0001	6.305	-0.240	12949796	11754810
		CD27	0.459	0.0005	3.705	-0.240	15345595	22278254
		TOX	0.389	<0.0001	4.679	-0.266	26885442	26885442
		CD160	0.350	0.0001	4.297	-0.458	25711213	22916009
		CD244	0.340	<0.0001	4.798	-0.251	15634901	28396665
		ZEB2	0.303	<0.0001	4.762	-0.165	26503445	26503446
		CCR5	0.204	0.0043	2.981	-0.568	22720226	9050881
		MMP9	1.7164	<0.0001	4.4987	-0.0088	26979530	28902848
		IQGAP1	1.2742	0.0002	3.9852	-0.2185	26252773	17950003
	inversely permissive	EOMES	4.0533	<0.0001	4.7282	-0.2156	20713880	25032686
		BATF	3.4560	0.0007	3.5700	-0.3773	26376615	25790189
		KLF4	1.3755	0.0380	2.2077	-0.0364	26977883	26372274
		ICOS	1.2651	0.0074	2.7812	-0.2228	24687957	20116985
		CXCR3	1.2182	0.0268	2.2624	-0.2124	26434630	24035365
		ETS1	0.9078	0.0002	4.0153	0.2169	23288305	21148801
		TGFBR2	0.8263	0.0001	4.1642	0.3311	12154374	23217625
		IL18RAP	0.7503	0.0122	2.5922	0.4205	27148488	27049306
		BCL11B	0.7488	0.0019	3.3185	0.3056	21878675	20660613
		TNF	0.6742	0.0055	2.8897	0.3435	18954521	20400885
		NFIL3	0.6712	0.0727	1.8224	0.2080	26539561	25768938
		SNRK	0.5830	0.0010	3.4779	0.1106	22874833	24498147
		LEF1	0.5553	<0.0001	5.1683	0.3496	20688898	24664171
		IFNG	0.5292	<0.0001	4.5764	0.2017	19451644	24454311
		JUN	0.3042	0.0161	2.4826	0.0804	17442952	10488148
		CD28	0.2785	0.0016	3.3208	0.3417	25550693	26945343

Supplemental Table S5. Comparison of validation assays to HIV-1 elite controllers. Pan-cancer DEGs were compared to DEGs identified from HIV-1 elite controllers (*n* = 81 patients and 98 controls). Many Pan-cancer DEGs are commonly modulated in expression, or have similar effects towards inducing T cell HIV-1 or cancer permissiveness. Pathways most associated with non-permissive genes included positive regulation of T cell gene translation, differentiation, activation, and proliferation, and response to cytokines. Pathways associated with permissive genes were regulation of cell surface receptor signaling, cytokine-receptor interactions, hepatitis B, and proteoglycans in cancer. Inversely permissive genes were also enriched in immune differentiation, but were also associated with auto-immune disease pathways. PMID, Pubmed ID; Avg.LogFC, average log fold-change; t-ratio, ratio divided by the standard error (GraphPad).

Table S6

Table S6: Immunotherapy resistance genes common to pan-cancer DEGs.

	pan-cancer		GENEx
	ptPBMC / cdPBMC	TIL/TIIC	BIOMARK
Hugo et al.	CXCL5 **MMP9** ESAM FPR2 PLCB4 ZMYND12	CRYAB FXYD3 ITGA3 KBTBD4 NRP1 RASGRP1 SERPINE1 SMPD2 TCF4 TRPV4	IL10 **MMP9** NFIL3
Rizvi et al.	APP **BRAF** F13A1 ITGB7 **LEF1** LEPR SIGLEC6 SLC40A1 SORL1 TAOK1 TNIK OPHN1	AGAP2 **BRAF** COL1A1 DIAPH1 EED EIF5 FRAS1 GNAI3 ITGA9 ITGB6 ITPKB LIMK1 MED13 NCAPD3 NRP1 RASGRP1 SPARCL1 TCF4 THOC2 TLR2 TP53 SEMA3C NLRC5	CD244 FASLG IKZF1 IL18RAP **LEF1** MKI67 STAT4 TOX GATA3 JAK1

Supplemental Table S6. Immunotherapy resistance genes common to pan-cancer DEGs. Published transcriptomic and genetic profiles of melanoma and NSCLC patients treated by anti-PD-1 therapy were compared to pan-cancer DEGs (Hugo and Rizvi refs found in main text). Pan-cancer columns are DEGs discovered from ccRCC training set and confirmed across five cancers. Genex BIOMARK column represents DEGs we validated on our validation cohort.

Table S7

Table S7: Pan-cancer and T cell DEG validation summary.

a) CD8 ptPBL upregulated DEGs validated by qRT-PCR

	microarray	Biomark HD
DEG	P value	P value
RUNX1	<0.0001	0.0233
BATF ф§	<0.0001	0.0007
EOMES ф	<0.0001	<0.0001
IKZF1 ∞†ф	<0.0001	0.0115
RUNX3 ф	<0.0001	0.0043
ETS1 ∞ф	0.0001	0.0047
TIGIT *	0.0001	0.0109
ICOS *∞	0.0002	0.0074
ZEB2 ф§	0.0006	0.0417
IFNG *ф§	0.0007	0.0698
MMP9 *∞‡ф§	0.0013	<0.0001
IRF1 ф§	0.0014	0.0423
PRDM1	0.0018	0.0004
CDA *ф§	0.0021	0.0540
KLF4 ф	0.0025	0.0380
MKI67 †∞	0.0032	0.0014
BCL6 ∞§	0.0057	0.0428
SELP §	0.0073	0.0737
STAT3 *§	0.0214	0.0002
TIMP1 *ф§	0.0244	0.0688
IL6ST *∞	0.0416	0.0072

b) CD8 ptPBL downregulated DEGs validated by qRT-PCR

	microarray	Biomark HD
DEG	P value	P value
SNRK *∞	<0.0001	0.0010
TGFBR2 *ф	<0.0001	0.0001
DGKA ∞§	0.0003	0.0022
TCF7 *∞§	0.0005	<0.0001
RORA *∞§	0.0006	0.0052
CD6 §	0.0009	0.0770
LEF1 *∞†ф§	0.0024	<0.0001
BCL11B *∞ф§	0.0024	0.0026
SMAD3 ∞§	0.0027	0.0374
MPHOSPH8 *§	0.0051	0.0700
SLK *∞	0.0051	0.0502
JUN *∞ф	0.0081	0.0161
SPTBN1 *∞	0.0106	0.0008
IL7R ∞ф	0.0250	0.0291
NT5E ∞§	0.0329	0.0272
CD69 *∞ф§	0.0398	0.0222
PIM2 *∞ф§	0.0410	0.0009
CD27 ∞ф§	0.0411	0.0005
IL23A *∞ф§	0.0423	0.0327
IQGAP1 *	0.0455	0.0320

c) PBMC upregulated DEGs validated by qRT-PCR

	microarray	Biomark HD
DEG	P value	P value
STAT3 *§	0.0214	0.0011

d) PBMC downregulated DEGs validated by qRT-PCR

	microarray	Biomark HD
DEG	P value	P value
SNRK *∞	<0.0001	0.0226
BCL11B *∞ф§	0.0024	0.0796
JUN *∞	0.0081	0.0090
IQGAP1 *∞	0.0455	0.0427

e) Other PBMC upregulated DEGs by qRT-PCR

	Biomark HD	
DEG	RCC / cd t ratio	P value
BTLA	2.9077	0.0060
DGKE *	1.7710	0.0846
IL17A	3.8160	0.0005
IL22	3.8160	0.0005
PDK4 *	2.0679	0.0455

f) Other PBMC downregulated DEGs by qRT-PCR

	Biomark HD	
DEG	RCC / cd t ratio	P value
CTLA-4	1.8752	0.0685
FOXO1 ∞ф§	2.6247	0.0124
FOXP3 ∞	1.7421	0.0896
LAG3 *	1.7141	0.0947
NFIL3 ∞‡ф	2.0489	0.0474
NOC2L	2.5649	0.0144
PDCD1 ∞	2.0897	0.0434
SPI1 ∞ф	2.0089	0.0517
STAT4 ф§	1.8043	0.0791
STAT6 ∞ф§	4.9879	<0.0001

* validated pan-cancer DEGs identified by this study
∞ top Biomark HD correlating genes
ф common to both HIV-1 and cancer resistance
§ common to bacterial infection by Song et al.
‡ common to immunotherapy resistance Hugo et al.
† common to immunotherapy resistance by Rizvi et al.
cd, control donor
pt, patient

Supplemental Table S7. Pan-cancer and T cell DEG validation summary. Table summarizing significant DEGs validated from microarrays using microfluidics qRT-PCR and new RCC cohort. Table also highlights DEGs most significantly correlating, and those common to studies HIV-1 resistance, bacterial resistance, and resistance to immunotherapy. Red are increased in expression, green are decreased in expression. (a-f) all DEGs validated from microarrays to qRT-PCR. (a) DEGs validated as upregulated in CD8+ T cells isolated from ptPBMC relative to those isolated from cdPBMC. (b) DEGs validated as downregulated in CD8+ T cells isolated from ptPBMC relative to those isolated from cdPBMC. (c) DEGs validated as upregulated in total ptPBMC relative to those isolated from cdPBMC. (d) DEGs validated as downregulated in total ptPBMC relative to those isolated from cdPBMC. (e) Other PBL DEGs observed as being

significantly upregulated by qRT-PCR. (f) Other PBL DEGs observed as being significantly upregulated by qRT-PCR. Symbols: *, validated pan-cancer DEGs identified by this study; ∞, top Biomark HD correlating genes; ф, common to both HIV-1 and cancer resistance; §, common to bacterial infection by Song et al.; ǂ, common to immunotherapy resistance Hugo et al.; †, common to immunotherapy resistance by Rizvi et al.

Table S8

Table S8: Spliceoforms of pan-cancer DEGs.

Isolate	Gene	Tot. No	Transcript Cluster ID	Group	PSR/Junction ID	Splicing Event	ANOVA	Splice Index	Splice Score
ptPBMC/TIIC	CD69	2	TC12001207.hg.1	Coding	PSR12015916.hg.1	Intron Retention	0.04458	-3.37	0.5
TIL/TIIC	CD69	2	TC12001207.hg.1	Coding	PSR12015916.hg.1	Intron Retention	0.04458	-3.37	0.5
ptPBMC/cdPBMC	CD69	1	TC12001207.hg.1	Coding	PSR12015916.hg.2	Intron Retention	0.0254	-4.24	0.69
ptPBMC/TIIC	IQGAP1	11	TC15000864.hg.1	Coding	PSR15008089.hg.1	Cassette Exon	0.04307	-4.52	0.22
TIL/TIIC	IQGAP1	3	TC15000864.hg.1	Coding	PSR15008089.hg.1	Cassette Exon	0.03493	-2.59	0.1
TIL/TIIC	IQGAP1	3	TC15000864.hg.1	Coding	PSR15008097.hg.1	Cassette Exon	0.00712	-2.56	0.11
ptPBMC/TIIC	IQGAP1	11	TC15000864.hg.1	Coding	PSR15008097.hg.1	Cassette Exon	0.00946	-2.29	0.02
ptPBMC/cdPBMC	IQGAP1	2	TC15000864.hg.1	Coding	PSR15008097.hg.2	Cassette Exon	0.03111	2.07	0.15
ptPBMC/TIIC	LAG3	4	TC12000091.hg.1	Coding	PSR12001036.hg.1	Intron Retention	0.00911	-4.14	0.75
TIL/TIIC	LAG3	5	TC12000091.hg.1	Coding	PSR12001036.hg.1	Intron Retention	0.01698	-3.58	0.64
ptPBMC/TIL	MMP9	4	TC20000363.hg.1	Coding	PSR20005253.hg.1	Cassette Exon	0.02365	6.88	0.32
ptPBMC/TIIC	MMP9	3	TC20000363.hg.1	Coding	PSR20005253.hg.1	Cassette Exon	0.04717	3.32	0.22
TIL/TIIC	MMP9	2	TC20000363.hg.1	Coding	PSR20005253.hg.1	Mutually Exclusive Exons*	0.00995	-2.07	0.22
ptPBMC/TIIC	MPHOSPH8	7	TC13000017.hg.1	Coding	PSR13000059.hg.1	Cassette Exon	0.00082	2.21	0.25
TIL/TIIC	MPHOSPH8	5	TC13000017.hg.1	Coding	PSR13000059.hg.1	Cassette Exon	0.01921	2.07	0.27
ptPBMC/TIIC	MPHOSPH8	7	TC13000017.hg.1	Coding	PSR13000063.hg.1	Cassette Exon	0.02955	2.81	0.16
TIL/TIIC	MPHOSPH8	5	TC13000017.hg.1	Coding	PSR13000063.hg.1	Cassette Exon	0.00483	2.69	0.15
ptPBMC/TIL	TCF7	3	TC05000657.hg.1	Coding	PSR05009040.hg.1	Cassette Exon	0.01458	-9.09	0.28
ptPBMC/TIIC	TCF7	44	TC05000657.hg.1	Coding	PSR05009040.hg.1	Cassette Exon	0.01231	-19.14	0.28
TIL/TIIC	TCF7	3	TC05000657.hg.1	Coding	PSR05009040.hg.1	Cassette Exon	0.00963	-2.11	0.1
ptPBMC/TIIC	TIGIT	5	TC03000588.hg.1	Coding	PSR03010797.hg.1	Alternative 5' Donor Site	0.04456	-2.75	0.28
TIL/TIIC	TIGIT	10	TC03000588.hg.1	Coding	PSR03010797.hg.1	Alternative 5' Donor Site	0.02218	-3.28	0.36
ptPBMC/TIIC	TIGIT	5	TC03000588.hg.1	Coding	PSR03010790.hg.1	Cassette Exon	0.03836	-7.71	0.14
TIL/TIIC	TIGIT	10	TC03000588.hg.1	Coding	PSR03010790.hg.1	Cassette Exon	0.04747	-7.88	0.07
ptPBMC/TIIC	TIMP1	3	TC0X000238.hg.1	Coding	PSR0X002817.hg.1	Intron Retention	0.00831	-3.55	0.64
TIL/TIIC	TIMP1	4	TC0X000238.hg.1	Coding	PSR0X002817.hg.1	Intron Retention	0.0153	-3.91	0.73

* difference in splicing event estimate

Supplemental Table S8. Spliceoforms of pan-cancer DEGs. TAC expression console was used with paired ccRCC isolates to define pan-cancer genes not only modified in overall gene expression, but also possibly affecting T cell fitness by being expressed as modified RNA isoforms. Only coding genes are represented in table. Tot. No. represents total number of significant isoforms present between isolates. PSR/Junction ID retained is matched significant isoform present across isolates. All other definitions can be found at: https://assets.thermofisher.com/TFS-Assets/LSG/manuals/tac_user_manual.pdf.

Table S9

Table S9: ptPBL DEGs correlating with MMP9 pathways

ptPBL DEG	Spearman r	95% CI	P val (two-tailed)
AAK1	0.1652	0.1173 to 0.2123	<0.0001
ABL1	0.1257	0.07731 to 0.1735	<0.0001
ACAP1	0.1408	0.09258 to 0.1884	<0.0001
ACTG1	0.1783	0.1306 to 0.2252	<0.0001
ACTL6A	0.1284	0.08008 to 0.1762	<0.0001
ACTN1	0.2775	0.2318 to 0.3220	<0.0001
ADGRE3	0.1213	0.07287 to 0.1691	<0.0001
ANGPT1	0.2402	0.1936 to 0.2857	<0.0001
APP	0.226	0.1792 to 0.2719	<0.0001
ARHGAP10	0.1125	0.06395 to 0.1604	<0.0001
ARHGEF6	0.1284	0.08002 to 0.1761	<0.0001
ARIH2	0.1247	0.07628 to 0.1725	<0.0001
ATM	0.1128	0.06429 to 0.1608	<0.0001
BACH2	0.1328	0.08451 to 0.1805	<0.0001
BCL2	0.1453	0.09710 to 0.1928	<0.0001
BCL2L1	0.1432	0.09506 to 0.1908	<0.0001
BLK	0.113	0.06451 to 0.1610	<0.0001
BMP6	0.1683	0.1204 to 0.2154	<0.0001
BMPR2	0.2239	0.1770 to 0.2698	<0.0001
BPI	0.1522	0.1041 to 0.1996	<0.0001
BRAF	0.1162	0.06771 to 0.1641	<0.0001
BTK	0.1841	0.1365 to 0.2309	<0.0001
CALD1	0.2234	0.1765 to 0.2693	<0.0001
CAMK4	0.117	0.06853 to 0.1649	<0.0001
CAMP	0.4261	0.3853 to 0.4653	<0.0001
CARD11	0.3902	0.3480 to 0.4309	<0.0001
CARD19	0.3019	0.2569 to 0.3457	<0.0001
CASP8AP2	0.1821	0.1344 to 0.2289	<0.0001
CBL	0.177	0.1292 to 0.2239	<0.0001
CCL5	0.4893	0.4513 to 0.5256	<0.0001
CCR4	0.09564	0.04701 to 0.1438	<0.0001
CD109	0.1074	0.05884 to 0.1554	<0.0001
CD151	0.2818	0.2362 to 0.3262	<0.0001
CD226	0.2096	0.1624 to 0.2559	<0.0001
CD27	0.3379	0.2939 to 0.3805	<0.0001
CD38	0.2256	0.1787 to 0.2715	<0.0001
CD3D	0.1969	0.1495 to 0.2434	<0.0001
CD3E	0.3216	0.2771 to 0.3647	<0.0001
CD3G	0.2001	0.1527 to 0.2465	<0.0001
CD5	0.1223	0.07387 to 0.1701	<0.0001
CD6	0.1182	0.06973 to 0.1661	<0.0001
CD69	0.2316	0.1848 to 0.2773	<0.0001
CD8B	0.3277	0.2834 to 0.3706	<0.0001
CD96	0.2595	0.2134 to 0.3045	<0.0001
CDK13	0.1625	0.1146 to 0.2097	<0.0001
CEACAM8	0.1251	0.07669 to 0.1729	<0.0001
CFL2	0.2125	0.1653 to 0.2586	<0.0001
CIITA	0.1206	0.07219 to 0.1685	<0.0001
CLEC1B	0.189	0.1414 to 0.2357	<0.0001
CLEC2D	0.1476	0.09942 to 0.1950	<0.0001
CLEC4D	0.181	0.1333 to 0.2278	<0.0001
CMIP	0.1047	0.05617 to 0.1528	<0.0001
COCH	0.2896	0.2441 to 0.3337	<0.0001
CREBBP	0.0991	0.05048 to 0.1472	<0.0001
CRISPLD2	0.1699	0.1220 to 0.2169	<0.0001
CSNK1G2	0.116	0.06757 to 0.1640	<0.0001
CSNK2A2	0.1445	0.09628 to 0.1920	<0.0001
CTSW	0.181	0.1333 to 0.2278	<0.0001
CUL1	0.1188	0.07032 to 0.1667	<0.0001
CXCL5	0.4589	0.4194 to 0.4966	<0.0001
DAB2	0.1744	0.1266 to 0.2214	<0.0001
DDX5	0.1309	0.08254 to 0.1786	<0.0001
DDX60	0.09845	0.04984 to 0.1466	<0.0001
DEFA1B	0.2007	0.1533 to 0.2471	<0.0001
DGKG	0.1537	0.1056 to 0.2010	<0.0001
DHX9	0.125	0.07656 to 0.1728	<0.0001
DPCD	0.2306	0.1838 to 0.2763	<0.0001
EGF	0.2901	0.2447 to 0.3342	<0.0001
EIF2AK2	0.1649	0.1170 to 0.2121	<0.0001
EIF4G1	0.1278	0.07944 to 0.1756	<0.0001
ELP1	0.2235	0.1766 to 0.2695	<0.0001
ELP2	0.251	0.2047 to 0.2963	<0.0001
EMB	0.1211	0.07270 to 0.1690	<0.0001
ENDOD1	0.1213	0.07287 to 0.1691	<0.0001
ENKUR	0.1235	0.07509 to 0.1713	<0.0001
ESAM	0.1996	0.1523 to 0.2461	<0.0001
F13A1	0.2785	0.2329 to 0.3230	<0.0001
FBXO31	0.1517	0.1036 to 0.1991	<0.0001
FKBP5	0.2683	0.2223 to 0.3130	<0.0001
FKBP8	0.226	0.1791 to 0.2719	<0.0001
FPR1	0.1587	0.1107 to 0.2060	<0.0001
FPR2	0.1376	0.08932 to 0.1852	<0.0001
FSTL1	0.3269	0.2826 to 0.3699	<0.0001
FUBP1	0.09781	0.04919 to 0.1460	<0.0001
GP1BA	0.2903	0.2449 to 0.3344	<0.0001
GP1BB	0.2101	0.1629 to 0.2563	<0.0001
GP5	0.1832	0.1355 to 0.2300	<0.0001
GP6	0.2743	0.2285 to 0.3189	<0.0001
GRB14	0.1564	0.1084 to 0.2037	<0.0001
GRK4	0.1283	0.07996 to 0.1761	<0.0001
GRK5	0.1303	0.08192 to 0.1780	<0.0001
HBA2	0.1096	0.06106 to 0.1576	<0.0001
HIST1H2AE	0.1139	0.06537 to 0.1618	<0.0001
HIST4H4	0.09753	0.04890 to 0.1457	<0.0001
HMGA1	0.1442	0.09604 to 0.1917	<0.0001
HNRNPU	0.1025	0.05392 to 0.1506	<0.0001
HSP90AA1	0.102	0.05340 to 0.1501	<0.0001
HSP90AB1	0.1254	0.07705 to 0.1732	<0.0001
HSP90AB3P	0.4366	0.3962 to 0.4753	<0.0001
HSP90B1	0.278	0.2323 to 0.3225	<0.0001
HSPA5	0.1548	0.1067 to 0.2021	<0.0001
HSPH1	0.2269	0.1800 to 0.2727	<0.0001
HYOU1	0.3092	0.2643 to 0.3527	<0.0001
IFI6	0.246	0.1995 to 0.2913	<0.0001
IGHA1	0.1745	0.1267 to 0.2214	<0.0001
IGKC	0.1454	0.09718 to 0.1928	<0.0001
IGKV1-17	0.1246	0.07619 to 0.1724	<0.0001
IGKV1-27	0.105	0.05645 to 0.1531	<0.0001
IGKV1D-33	0.1041	0.05548 to 0.1521	<0.0001
IL23A	0.4213	0.3803 to 0.4607	<0.0001
IL3RA	0.1162	0.06776 to 0.1642	<0.0001
IL6ST	0.2931	0.2478 to 0.3371	<0.0001
IL7R	0.2182	0.1711 to 0.2642	<0.0001
ILF3	0.1085	0.05993 to 0.1565	<0.0001
INPP5D	0.2349	0.1882 to 0.2806	<0.0001
IQGAP1	0.1597	0.1117 to 0.2069	<0.0001
IRF4	0.3441	0.3002 to 0.3864	<0.0001
ITGA2B	0.2776	0.2319 to 0.3221	<0.0001
ITGA6	0.2524	0.2061 to 0.2976	<0.0001
ITGB3	0.2709	0.2251 to 0.3156	<0.0001
ITGB5	0.3007	0.2556 to 0.3445	<0.0001
ITGB7	0.2952	0.2500 to 0.3392	<0.0001
ITK	0.1883	0.1407 to 0.2350	<0.0001
JAM3	0.28	0.2344 to 0.3244	<0.0001
KPNA4	0.2352	0.1885 to 0.2808	<0.0001
KTN1	0.1186	0.07020 to 0.1665	<0.0001
LAX1	0.1223	0.07393 to 0.1702	<0.0001
LCN2	0.1495	0.1014 to 0.1970	<0.0001
LDLRAP1	0.1702	0.1223 to 0.2172	<0.0001
LEF1	0.1593	0.1113 to 0.2066	<0.0001
LEPR	0.1092	0.06070 to 0.1573	<0.0001
LGALS3BP	0.3407	0.2968 to 0.3832	<0.0001
LIMS1	0.1339	0.08561 to 0.1816	<0.0001
LTB	0.3474	0.3037 to 0.3897	<0.0001
LTBP1	0.2859	0.2405 to 0.3302	<0.0001
LY9	0.2788	0.2331 to 0.3232	<0.0001
MAL	0.1895	0.1419 to 0.2362	<0.0001
MALT1	0.3924	0.3503 to 0.4330	<0.0001
MAP3K9	0.1571	0.1091 to 0.2044	<0.0001
MAP4K1	0.1672	0.1193 to 0.2143	<0.0001
MAPKAP1	0.1886	0.1411 to 0.2353	<0.0001
MAX	0.1793	0.1316 to 0.2262	<0.0001
MCM7	0.1202	0.07173 to 0.1680	<0.0001
MIA3	0.1719	0.1241 to 0.2189	<0.0001
MMP12	0.3964	0.3544 to 0.4368	<0.0001
MMRN1	0.301	0.2559 to 0.3448	<0.0001
MPP1	0.1437	0.09556 to 0.1913	<0.0001
MSN	0.2979	0.2527 to 0.3417	<0.0001
MTMR1	0.158	0.1100 to 0.2053	<0.0001
MTOR	0.1562	0.1082 to 0.2035	<0.0001
MTURN	0.1745	0.1267 to 0.2215	<0.0001
MX1	0.1738	0.1260 to 0.2208	<0.0001
MXD1	0.1364	0.08809 to 0.1840	<0.0001
MYL9	0.2515	0.2052 to 0.2967	<0.0001
MYLK	0.2052	0.1579 to 0.2515	<0.0001
NCOA3	0.1446	0.09639 to 0.1921	<0.0001
NCOR1	0.1845	0.1369 to 0.2313	<0.0001
NELL2	0.3085	0.2636 to 0.3520	<0.0001
NFE2	0.1894	0.1418 to 0.2360	<0.0001
NLK	0.1767	0.1290 to 0.2236	<0.0001
NLRC4	0.2827	0.2372 to 0.3271	<0.0001
NOG	0.1755	0.1278 to 0.2225	<0.0001
NPTN	0.1086	0.06603 to 0.1566	<0.0001
NRG1	0.1024	0.05378 to 0.1505	<0.0001
NT5E	0.0967	0.04807 to 0.1449	<0.0001
OAS2	0.1783	0.1306 to 0.2252	<0.0001
P2RX1	0.09706	0.04843 to 0.1452	<0.0001
PAG1	0.1221	0.07371 to 0.1700	<0.0001
PANX1	0.2219	0.1749 to 0.2678	<0.0001
PDCD4	0.2204	0.1734 to 0.2663	<0.0001
PDCD6IP	0.1716	0.1238 to 0.2186	<0.0001
PDGFA	0.3293	0.2850 to 0.3721	<0.0001
PDLIM1	0.1846	0.1369 to 0.2313	<0.0001
PF4	0.5942	0.5617 to 0.6249	<0.0001
PF4V1	0.2917	0.2463 to 0.3357	<0.0001
PGLYRP1	0.1955	0.1481 to 0.2421	<0.0001
PIK3CA	0.1259	0.07750 to 0.1737	<0.0001
PIK3CD	0.1426	0.09439 to 0.1901	<0.0001
PIM2	0.1503	0.1022 to 0.1977	<0.0001
PKHD1L1	0.3729	0.3301 to 0.4142	<0.0001
PLCB4	0.0971	0.04848 to 0.1453	<0.0001
PMAIP1	0.1914	0.1439 to 0.2381	<0.0001
POMK	0.1193	0.07082 to 0.1671	<0.0001
PPBP	0.3496	0.3060 to 0.3918	<0.0001
PPM1A	0.2027	0.1554 to 0.2491	<0.0001
PPP3CC	0.214	0.1669 to 0.2601	<0.0001
PRDX6	0.1473	0.09917 to 0.1948	<0.0001
PREX1	0.09517	0.04653 to 0.1434	<0.0001
PRKAR2B	0.09618	0.04754 to 0.1444	<0.0001
PRKCH	0.1598	0.1118 to 0.2070	<0.0001
PROS1	0.2561	0.2098 to 0.3011	<0.0001
RNF11	0.1171	0.06864 to 0.1650	<0.0001
RPL30	0.1682	0.1203 to 0.2153	<0.0001
RUNX2	0.1549	0.1069 to 0.2022	<0.0001
S100P	0.1018	0.05324 to 0.1499	<0.0001
SBK1	0.113	0.06452 to 0.1610	<0.0001
SDC4	0.2259	0.1790 to 0.2717	<0.0001
SELP	0.4909	0.4529 to 0.5271	<0.0001
SELPLG	0.2006	0.1533 to 0.2471	<0.0001
SERPINB9	0.1173	0.06885 to 0.1652	<0.0001
SFPQ	0.17	0.1221 to 0.2170	<0.0001
SIRPG	0.3591	0.3158 to 0.4009	<0.0001
SKAP1	0.1102	0.06165 to 0.1582	<0.0001
SLA2	0.1851	0.1375 to 0.2319	<0.0001
SLK	0.1386	0.09037 to 0.1862	<0.0001
SMAD3	0.1924	0.1449 to 0.2390	<0.0001
SNCA	0.1509	0.1028 to 0.1983	<0.0001
SNRK	0.1924	0.1449 to 0.2390	<0.0001
SP100	0.2343	0.1875 to 0.2795	<0.0001
SPARC	0.3341	0.2900 to 0.3768	<0.0001
SPOCK2	0.2575	0.2113 to 0.3026	<0.0001
SPTBN1	0.1637	0.1158 to 0.2109	<0.0001
STIP1	0.1336	0.08532 to 0.1813	<0.0001
TAL1	0.1103	0.06173 to 0.1583	<0.0001
TAOK1	0.1726	0.1248 to 0.2196	<0.0001
TAP2	0.1041	0.05548 to 0.1521	<0.0001
TBP	0.1518	0.1037 to 0.1992	<0.0001
TCF7	0.1005	0.05192 to 0.1486	<0.0001
TFPI	0.3141	0.2694 to 0.3575	<0.0001
TGFB1	0.427	0.3862 to 0.4661	<0.0001
TGFB1I1	0.223	0.1760 to 0.2689	<0.0001
TGFBR2	0.2797	0.2340 to 0.3241	<0.0001
TGFBRAP1	0.1291	0.08073 to 0.1768	<0.0001
THBS1	0.411	0.3696 to 0.4508	<0.0001
TIMP1	0.4868	0.4486 to 0.5232	<0.0001
TLR10	0.3184	0.2738 to 0.3617	<0.0001
TMEM189	0.1489	0.1007 to 0.1963	<0.0001
TNFRSF17	0.2181	0.1711 to 0.2641	<0.0001
TNFSF10	0.3512	0.3076 to 0.3933	<0.0001
TNFSF4	0.1943	0.1468 to 0.2408	<0.0001
TNFSF8	0.1548	0.1067 to 0.2021	<0.0001
TNIK	0.1713	0.1235 to 0.2183	<0.0001
TOM1L1	0.1039	0.05532 to 0.1520	<0.0001
TPM1	0.1612	0.1132 to 0.2084	<0.0001
TPM4	0.1078	0.05929 to 0.1559	<0.0001
TPR	0.1293	0.08098 to 0.1771	<0.0001
TRAF5	0.2889	0.2435 to 0.3330	<0.0001
TRAM2	0.1864	0.1388 to 0.2331	<0.0001
TREML1	0.3034	0.2583 to 0.3471	<0.0001
TRIM28	0.09707	0.04845 to 0.1452	<0.0001
TRIM40	0.2499	0.2035 to 0.2952	<0.0001
TRIM52	0.1621	0.1142 to 0.2093	<0.0001
TRIO	0.1362	0.08790 to 0.1838	<0.0001
TUBA4A	0.1988	0.1514 to 0.2453	<0.0001
TUBA8	0.2724	0.2265 to 0.3170	<0.0001
TUBB1	0.237	0.1904 to 0.2826	<0.0001
TUBB3	0.2206	0.1736 to 0.2666	<0.0001
UBASH3A	0.1697	0.1218 to 0.2167	<0.0001
USP31	0.1147	0.06624 to 0.1627	<0.0001
VDR	0.1813	0.1336 to 0.2281	<0.0001
VEGFC	0.3588	0.3155 to 0.4007	<0.0001
VIL1	0.1826	0.1350 to 0.2294	<0.0001
VNN1	0.09706	0.04843 to 0.1452	<0.0001
WASF3	0.1144	0.06589 to 0.1623	<0.0001
YWHAE	0.1285	0.08015 to 0.1763	<0.0001
YWHAZ	0.1238	0.07543 to 0.1717	<0.0001
PARP1	0.09306	0.04440 to 0.1413	0.0001
CHD7	0.09161	0.04295 to 0.1398	0.0002
CYSTM1	0.09119	0.04252 to 0.1394	0.0002
SH3YL1	0.09095	0.04228 to 0.1392	0.0002
ASAP2	0.09057	0.04190 to 0.1388	0.0002
THRA	0.0904	0.04172 to 0.1386	0.0002
PDE4A	0.08989	0.04121 to 0.1381	0.0002
CXCR1	0.08889	0.04021 to 0.1372	0.0002
ATF6	0.08856	0.03987 to 0.1368	0.0002
SIGLEC6	0.08848	0.03980 to 0.1367	0.0003
GLUL	0.0884	0.03971 to 0.1367	0.0003
VCL	0.08787	0.03918 to 0.1361	0.0003
PADI4	0.08719	0.03849 to 0.1355	0.0003
OPHN1	0.0863	0.03760 to 0.1346	0.0004
ALOX12	0.08616	0.03746 to 0.1345	0.0004
DEFA1	0.08613	0.03743 to 0.1344	0.0004
IGKV2D-40	0.08613	0.03743 to 0.1344	0.0004
MB21D1	0.08613	0.03743 to 0.1344	0.0004
FCRL1	0.08603	0.03733 to 0.1343	0.0004
ERAP1	0.08572	0.03702 to 0.1340	0.0004
RNF217	0.08572	0.03702 to 0.1340	0.0004
GRAP2	0.08471	0.03600 to 0.1330	0.0005
LY6G6F	0.08465	0.03594 to 0.1330	0.0005
SCD	0.08452	0.03581 to 0.1328	0.0005
SOD2	0.08422	0.03551 to 0.1325	0.0005
RPAP3	0.08406	0.03535 to 0.1324	0.0005
HCP5	0.08226	0.03354 to 0.1306	0.0007
TMC8	0.08226	0.03354 to 0.1306	0.0007
DOCK11	0.0822	0.03348 to 0.1305	0.0007
ABCC4	0.08078	0.03205 to 0.1291	0.0008
IGKV3-11	0.08078	0.03205 to 0.1291	0.0008
LRP12	0.08078	0.03205 to 0.1291	0.0008
MFSD1	0.08078	0.03205 to 0.1291	0.0008
POLR3G	0.08064	0.03190 to 0.1290	0.0009
SKAP2	0.0802	0.03146 to 0.1286	0.0009
DNM3	0.07997	0.03123 to 0.1283	0.0009
MDM4	0.07976	0.03102 to 0.1281	0.001
TSPAN2	0.07913	0.03039 to 0.1275	0.0011
DGKA	0.07911	0.03037 to 0.1275	0.0011
SUPT6H	0.07908	0.03034 to 0.1274	0.0011
NSD1	0.07832	0.02958 to 0.1267	0.0012
GNAZ	0.07668	0.02793 to 0.1251	0.0015
KIAA2026	0.07551	0.02676 to 0.1239	0.0018
ABCC3	0.07407	0.02530 to 0.1225	0.0022
POLR2A	0.07287	0.02410 to 0.1213	0.0026
CYP4F3	0.07216	0.02339 to 0.1206	0.0029
NOSIP	0.07209	0.02331 to 0.1205	0.0029
SLAMF1	0.07177	0.02299 to 0.1202	0.003
IGKV1D-16	0.07152	0.02274 to 0.1200	0.0031
NOLC1	0.07146	0.02268 to 0.1199	0.0031
JUN	0.07138	0.02260 to 0.1198	0.0032
ARHGEF12	0.07098	0.02220 to 0.1194	0.0033
VEZF1	0.07028	0.02150 to 0.1187	0.0037
UFL1	0.07013	0.02135 to 0.1186	0.0037
ARHGAP15	0.06967	0.02088 to 0.1181	0.004
IGKV1-5	0.06896	0.02017 to 0.1174	0.0044
EIF2AK3	0.06887	0.02008 to 0.1173	0.0044
SH3BGRL3	0.06887	0.02008 to 0.1173	0.0044
POU4F3	0.06813	0.01934 to 0.1166	0.0049
ANXA11	0.06768	0.01889 to 0.1162	0.0051
SIN3A	0.06651	0.01771 to 0.1150	0.006
MAP1LC3B	0.06582	0.01701 to 0.1143	0.0065
ZC3HAV1	0.06575	0.01695 to 0.1142	0.0066
CAVIN2	0.06571	0.01691 to 0.1142	0.0066
TMF1	0.06439	0.01558 to 0.1129	0.0078
SNX25	0.06435	0.01554 to 0.1128	0.0078
TTC3	0.06256	0.01374 to 0.1111	0.0097
PROK2	0.06246	0.01364 to 0.1110	0.0098
MEIS1	0.06172	0.01290 to 0.1102	0.0108
RPTOR	0.06097	0.01215 to 0.1095	0.0117
CMTM5	0.06059	0.01177 to 0.1091	0.0123
CYP4F11	0.06059	0.01177 to 0.1091	0.0123
DEFB129	0.06059	0.01177 to 0.1091	0.0123
MYCT1	0.06059	0.01177 to 0.1091	0.0123
OR2W3	0.06059	0.01177 to 0.1091	0.0123
SIAE	0.06059	0.01177 to 0.1091	0.0123
ZEB2	0.06046	0.01164 to 0.1090	0.0125
LAPTM4B	0.06027	0.01145 to 0.1088	0.0128
ARHGAP6	0.05877	0.009941 to 0.1073	0.0152
ABLIM3	0.05862	0.009796 to 0.1072	0.0154
SLC12A2	0.05845	0.009616 to 0.1070	0.0157
SNAP23	0.05728	0.008451 to 0.1058	0.0179
HERC6	0.05512	0.006281 to 0.1037	0.0228
CLK1	0.05446	0.005619 to 0.1030	0.0244
CDA	0.05418	0.005334 to 0.1028	0.0252
P2RY8	0.05418	0.005334 to 0.1028	0.0252
PEAR1	0.05418	0.005334 to 0.1028	0.0252
VSIG1	0.05418	0.005334 to 0.1028	0.0252
STRN	0.05342	0.004577 to 0.1020	0.0273
SORL1	0.05302	0.004169 to 0.1016	0.0285
CTSA	0.05282	0.003970 to 0.1014	0.0291
HBG2	0.05282	0.003970 to 0.1014	0.0291
TBXA2R	0.05276	0.003913 to 0.1014	0.0293
VSTM1	0.05273	0.003880 to 0.1013	0.0294
PLCG1	0.05189	0.003044 to 0.1005	0.032
UBE4A	0.05174	0.002888 to 0.1003	0.0326
CETP	0.05097	0.002113 to 0.09957	0.0352
MGAM	0.05097	0.002113 to 0.09957	0.0352
MOB1B	0.05097	0.002113 to 0.09957	0.0352
ZDHHC15	0.05097	0.002113 to 0.09957	0.0352
THRAP3	0.05081	0.001960 to 0.09942	0.0358
NEXN	0.0505	0.001649 to 0.09911	0.0369
FMNL1	0.05008	0.001221 to 0.09869	0.0386
MYL4	0.05008	0.001221 to 0.09869	0.0386
DOCK9	0.04952	0.0006672 to 0.09814	0.0408
ST3GAL3	0.04778	-0.001078 to 0.09641	0.0484

Supplemental Table S9. Correlation of ptPBL DEGs with MMP9 pathways. Spearman correlation analyses were performed on pathDIP-identified significantly enriched pathways that include MMP-9, and other associated ccRCC ptPBL DEGs (Graphpad).

Supplemental Methods for:

Failed immune responses across multiple pathologies share pan-tumor and circulating lymphocytic targets

Study design

This is a study of renal cancer patients who underwent resection for stage I-IV RCC at the CHUM (Montreal, Quebec, Canada), between 2013 and 2017. Written and informed consent procedures were approved by the CHUM research ethics board (REB). Informed consent was obtained from all subjects for participation in the CHUM kidney biobank (CHUM ref no. SL07.053) prior to the collection of specimens, and all methods were performed in accordance with the relevant guidelines and regulations. Clinical patient data was randomly numbered for complete anonymity. Training cohort and validation cohort had similar overall clinicopathological parameters (Supplemental Table 1), with exception that all training cohort patients were ccRCC, while a few pRCC and RCC patients were included in the validation cohort. The TCGA KIRC ccRCC RNA-seq datasets and clinical files used for analysis of single prognostic and synergistic prognostic DEGs (n = 534 tumor and n = 72 normal), were downloaded from http://gdac.broadinstitute.org/ on 02/12/2016. Pan-cancer, MAS5-normalized patient cohort GEO, the EGA and TCGA datasets including lung (n = 2,435), breast (n = 5,143), gastric (n = 2,183), and ovarian (n = 1,816) cancers, were derived from http://kmplot.com/. DEG protein profiles in cells and across 17 cancers were derived from https://www.proteinatlas.org/. For comparison of our DEGs to cancer immunotherapy resistance genes, we used two datasets, including a transcriptomic dataset from melanoma patients treated with anti-PD-1 therapy (n = 38) (1), in addition to a genetic

dataset from NSCLC patients treated with anti-PD-1 therapy (n = 31) (2). To compare our DEGs the effects of HIV-1 infection, we used a HIV-1 elite controllers dataset (n = 81 patient, n = 98 controls) (3). For comparison of DEGs to bacterial infection induced effects, we used four including generalized bacterial infection, sepsis, and specific infection by *Staphylococcus aureus* and *Escherichia coli* (*n* = 157 cases, *n* = 157 controls) (4).

Rapid RNA extraction from $CD8^+$ and $CD19^+$ immune cells

To avoid ischemia effects on RNA and proteins, tissue specimens and paired patient blood were kept on ice during immediate transport following surgical extraction, from operating rooms to pathology by a specialized research technician. Expert renal pathologists immediately classified and selected experimental tissues (i.e., tumor and normal adjacent tissues distant from tumor margins), and according to the defined guidelines from the WHO 2004 and the WHO 2016. Selected specimens were kept on ice during direct transport from pathology to TIL extraction laboratories. For the isolation of TILs and TIICs from freshly resected kidney tumors and normal adjacent tissues, cold tissues were homogenized using three consecutive cycles of the h_tumor_01 program of the gentleMACS™ Dissociator (Miltenyi Biotec, USA), and resulting cellular suspensions were passed through a 0.45 µm filter fit onto a 50 mL falcon tubes (Fisher), were pelleted by centrifugation (4 °C, 10 min, 300 g), and were subjected to Ficoll gradient separating lymphocytes from tumoral material (Lymphocyte separation medium; WISENT Bioproducts) followed by an additional two 50 mL PBS washes prior to cell pelleting by centrifugation (4 °C, 10 min, 300 g). 40 mL of blood from patients and matched control

donors were treated alongside tumors, via dilution in PBS for Ficoll gradient separation of immune cells (Lymphocyte separation medium; WISENT Bioproducts), pelleting of cells (4 °C, 10 min, 300 g), and followed by two additional 50 mL PBS washes prior to cell pelleting by centrifugation. Cell pellets were resuspended in EasySep™ Buffer (STEMCELL Technologies), and cells were counted and resuspended at appropriate dilutions for extraction using Human CD8 and CD19 Positive Selection Kits (STEMCELL Technologies), used as recommended by the manufacturer for the rapid isolation of $CD8^+$ and $CD19^+$ immune cells. Total RNA was purified using QIAshredder cell-lysate homogenizers followed by the RNeasy Plus Micro Kit (QIAGEN). The quality of the total RNA was evaluated with the RNA 6000 nano LabChip kit on an Agilent 2100 Bioanalyzer system (Agilent Technologies).

Flow cytometry

Efficiency of isolation of various immune cell subsets from tumors was quality tested using flow cytometry (**Supplemental figure S2**). Cells were counted and resuspended in PBS for transfer to 5 mL polystyrene round bottom FACS tubes (Falcon) where non-specific binding sites were blocked with human gamma globulin (Jackson ImmunoResearch) and dead cells were labeled for flow cytometry-mediated elimination using a LIVE/DEAD fixable Aqua Dead Cell Stain Kit (Life technologies) for 20 min at 4 °C. Following a cold PBS wash and centrifugation (4 °C, 5 min, 300 g), cells were resuspended in cold FACS buffer (PBS containing 0.5% BSA and 0.1% NaN_3) and were stained for 30 min at 4 °C with the following titrated monoclonal antibodies, α-CD45-PE-Cy7 (clone HI30), α-CD8-PE-Cy5 (clone RPA-T8), α-CD4-APC-H7 (clone L200), α-CD19-AF700 (clone HIB19),

and α-CD11c-APC (clone B-ly6) (BD Biosciences). Clones chosen were recommended by STEMCELL as these are not the same clones used in magnetic beads antibody separation mixtures otherwise interfering with flow cytometry antibodies. Cells were then washed with, and resuspended in cold FACS buffer for flow cytometry analysis. In multi-parametric FACS analyses, compensation beads (BD Biosciences) stained in parallel to cells were used to compensate for fluorescence spill over. Flow cytometry data was acquired using an LSR Fortessa cell analyzer with DIVA software (BD Biosciences) and data was analyzed using FlowJo V10 software.

Microarrays

Microarray experiments were performed using the GeneChip® HTA 2.0 (Affymetrix, Santa Clara, CA). This comprehensive array interrogates 44,699 protein-coding genes and 22,829 non-protein coding genes with approximately ten probes per exon and four probes per exon-exon splice junction. 1 ng of total RNA for each sample was processed using the Affymetrix GeneChip WT Pico Reagent Kit. This kit uses a reverse transcription priming method that specifically primes non-ribosomal RNA, including both poly(A) and non-poly(A) mRNA, and is used to generate sense-stranded cDNA. 5.5 µg of the single-stranded cDNA was then fragmented and labeled using the Affymetrix GeneChip WT Terminal Labeling Kit and it this product was hybridized onto the chip. The entire hybridization procedure was performed using the Affymetrix GeneChip system according to the manufacturer's recommendations. Test GeneChip® HTA 2.0 microarrays and GeneChip WT Pico Reagent kits were kindly donated by Peter Graf (Affymetrix). The hybridization was evaluated using the Affymetrix GeneChip

Command Console Software (AGCC) and the quality of the chips was assessed using the Affymetrix Expression Console. Normalization and QC analysis: The data obtained was normalized using Partek Genomics Suite™ 6.6 (Partek, St. Louis, Missouri). GC content adjustment, background adjustment, quantile normalization and mean probe set summarization were performed using the Robust Multichip Average (RMA) algorithm. Quality control analysis was then performed and included: QC metrics (pos vs. neg area under curve (AUC), all probe set mean absolute deviation (MAD) residual mean, all probe set relative log expression (RLE) mean, hybridization controls (BAC spike), synthesis controls (poly(A) spike), and log expression signal box plots), signal histograms, and principle component analysis (PCA). RNA expression analysis: Transcripts found to be significantly differentially expressed between groups, i.e., with p-values ≤ 0.05 and fold change cutoff of ≥1.5 (using analysis of variance (ANOVA) with Fisher's Least Significant Difference (LSD) posttest). 4-way Venn diagrams generated to demonstrate DEG overlaps from microarrays were created using http://www.interactivenn.net/ (5).

Real-Time quantitative PCR microfluidics gene expression analysis

cDNA was synthesized using the High-Capacity Reverse Transcription Kit with RNase Inhibitor (Life Technologies) (25˚C for 10 min, 37˚C for 120 min, 85˚C for 5 min). The produced cDNA was subjected to gene-specific preamplification using Taqman Preamp MasterMix (Applied Biosystems) and 96 pooled TaqMan Assays (Assay IDs are listed in **Supplemental table S4**) (Applied Biosystems) at final concentration 0.2X (95˚ C for 10 min, followed by 16 cycles of 95˚C for 15 s and 60˚C for 4 min). The preamplified cDNA was diluted 5-fold in DNA suspension buffer (Teknova) and was mixed with

TaqMan Universal PCR Master mix (Life Technologies) and 20X GE sample loading reagent (Fluidigm). 20X Taqman assays were diluted 1:1 with 2X assay loading buffer (Fluidigm). Samples and Taqman assays mixtures were loaded onto a primed 96.96 Dynamic Array chip (Fluidigm). The chip was loaded into the IFC Controller, where each sample was mixed with each assay in every possible combination (a total of 9,216 reactions). The chip was transferred in a Biomark (Fluidigm) for real-time PCR amplification and fluorescence acquisition using single probe (FAM-MGB, reference: ROX) settings and the default hot-start protocol with 40 cycles. Cycle thresholds (Ct) were calculated using the Fluidigm BioMark software and further analysis was carried out using GenEx software (MultiD Analyses, http://www.multid.se). Five endogenous control genes were included in each Fluidigm run and the stability of endogenous control genes across all experimental samples was evaluated applying the NormFinder algorithm in GenEx. The geometric mean expression of the four most stable endogenous control genes (IPO8, GUSB, PGK1 and POL2RA) was used for normalization. Relative expression (2-Δct) values were log2 transformed for subsequent analyses. Unsupervised hierarchical clustering was performed using the in heatmap2 function in R on mean-centered –ΔCt expression values applying the Euclidean distance metric and complete linkage clustering method (https://www.rdocumentation.org/packages/gplots/versions/3.0.1/topics/heatmap.2).

PCA biplots were created on –ΔCt values using the programming language R and function biplot (http://stat.ethz.ch/R-manual/R-devel/library/stats/html/biplot.princomp.html). Combination testing for revealing smaller sets of patient stratifying pan-cancer genes was performed by PCA testing for patient

stratifying combinations of DEGs that were most significantly modulated in expression, correlating, or anti-correlating in ptPBLs versus cdPBLs.

Statistical analysis

For the training ccRCC cohort, a sample size of *n* = 5 paired patient TILs, TIICs, and PBLs was determined as having above 0.9 power according to the GeneChip Human Transcriptome Array 2.0 manufacturer guidelines (Affymetrix, Thermo Fisher Scientific). Training set microarrays power calculations by the manufacturer used an inference of means calculation from https://www.stat.ubc.ca/~rollin/stats/ssize/n2. Multiple hypothesis test correction was performed using the FDR Benjamini–Hochberg step-up procedure. For the RCC validation cohort (*n* = 74), power analysis determined that a minimal sample size of *n* = 62 to reach a power of 0.80 at α = 0.05 (two-tailed) (G*Power ver. 3.1.9.2; Universitat Düsseldorf, Germany). For algorithms used, statistical methodology for algorithms is described within scripts and https://www.biostars.org/p/153013/. Limma and survival packages for R are used for single and synergistic ccRCC prognostic algorithms. Dendrogram, heatmap and PCA unsupervised algorithms used the Euclidean distance metric and complete linkage clustering method. Correlogram algorithm uses the R corrplot library, and was created from http://www.sthda.com/, using r-project corrplot and vignette packages. Binomial correlations for testing of validated DEGs against clinical patient parameters used two-tailed nonparametric Spearman correlation with 95% CI (Prism V6.01, GraphPad). An unpaired 2-tailed student's t test with FDR of 1% was used to compare two groups, and two-way ANOVA (with Sidak's multiple-comparisons test) and 95% CI was used for multiple comparisons. Pathway enrichment analysis results

were adjusted for multiple testing by applying FDR and Bonferroni methods. *P*-values of less than 0.05 were considered to indicate a statistically significant difference.

Prognostic Signature Validation and gene expression analysis

Kaplan Meier plotter was used to validate the prognostic value of the ICP signature, and to assess ICP gene expression modulation between tumors and normal tissues. Gene ID symbols were mapped to Affymetrix probes from GEO, EGA and TCGA datasets, and their mean expression was used to assess OS. For K-M, default settings were used with auto select best cutoff and best specific probes (JetSet probes). The 2017 version of Kaplan Meier plotter contains information on 54,675 genes for survival, including 2,437 lung, 5,143 breast, 1,065 gastric, and 1,816 ovarian cancer patients with mean follow-up times of 49, 69, 33, and 40 months, respectively.

Protein-Protein Interaction Network and Pathway Enrichment Analysis, and pan-cancer MMP-9 PPI networks

To test validity of performing in depth analyses on DEG datasets, online search engine STRING: functional protein association networks; https://string-db.org/) was first used to observe PPIs and PPI enrichment values. Then, top 200 pan-cancer DEGs and all ccRCC ptPBLs were subjected to comprehensive pathway enrichment analysis using pathDIP ver. 3 (http://ophid.utoronto.ca/pathDIP) (6). Default settings were used, with extended pathway associations (combining literature curated core pathways with associations predicted using physical protein interactions with minimum confidence levels of 0.99). Lists were also used to retrieve physical protein interactions and explore

biologically relevant links. IID ver. 04-2018 (http://ophid.utoronto.ca/iid) was used to map identified biomarkers to proteins and retrieve their interacting partners (7). Default settings were used, and interactions among partners of query proteins, source information (detection methods, PubMed IDs, reporting databases), and tissue information (presence/absence of interactions in selected tissues) were included. Corresponding networks were visualized using NAViGaTOR ver. 3 (http://ophid.utoronto.ca/navigator) (8).

For MMP-9 PPI networks: For PPI networks, 216 human PPIs for MMP-9 were obtained from IID (version 04-2018), 205 of which have proteins mapping to the gene expression data. Furthermore, 3,880 PPIs among interactors of MMP-9 were found, out of which, 3,776 PPIs were mapped to gene expression data. All of these PPIs were annotated with differential gene-coexpression and their normal or cancer specificity across thirteen different tissues (6). For differential gene co-expression networks, raw gene expression profiles for 1,013 non-malignant (N) and 1,788 tumor (T) pre-treatment patient samples were obtained from GEO. These data cover thirteen tissue-cancers, comprising: breast (86 N, 93 T), cervical (30 N, 52 T), colorectal (117 N, 345 T), endometrial (21 N, 58 T), esophageal (132 N, 159 T), renal (89 N,111 T renal), liver (20 N, 20 T), lung (188 N, 510 T), mouth (oral cavity and tongue; 67 N, 70 T), ovarian (49 N, 71 T), pancreatic (61 N, 73 T), prostate (96 N, 143 T), and thyroid (57 N, 84 T). GEO Accession Numbers of sample source datasets are as follows, (downloaded in 11/2012): GSE19383, GSE26910, GSE3744, GSE5764, GSE20437, GSE5364, GSE5462, GSE6883, GSE9574, GSE9750, GSE20916, GSE8671, GSE41258, GSE5364, GSE11024, GSE14762, GSE8271, GSE6280, GSE6344, GSE781, GSE6280, GSE6344,

GSE781, GSE29721, GSE14520, GSE10245, GSE19188, GSE28571, GSE31210, GSE31908, GSE10072, GSE31908, GSE5364, GSE7670, GSE31908, GSE14407, GSE15578, GSE18520, GSE19383, GSE36668, GSE38666, GSE15471, GSE16515, GSE22780, GSE17951, GSE32448, GSE32982, GSE3325, GSE6956, GSE29265, GSE3467, GSE3678, GSE6004, GSE27155, GSE5364; (downloaded 01/2016): GSE17025, GSE20347, GSE23400, GSE29001, GSE30784, GSE31056, GSE33426, GSE38129, GSE53757, GSE64985, GSE7305, GSE7307, GSE7803). Due to the lower sensitivity of co-expression (i.e., pairwise correlation) to batch effects relative to expression analysis, all samples were normalized using the MAS5 function implemented in Affy package (1.48.0) in R (9). For differentially co-expressed PPIs, for each pair of N and T samples in tissue-cancer datasets, their relevant co-expression matrices (i.e., ρ_N and ρ_T) were calculated using Pearson Correlation Coefficient. Absolute values of the difference between these two matrices as the differential co-expression matrix (i.e., $Diff_{(N,T)}$) were used. For each dataset, PPIs whose corresponding gene pair were among the top 1% of values in $Diff_{(N,T)}$ were annotated as differential PPIs in that particular tissue-cancer dataset. For MMP-9, we found 106 PPIs (out of 205) and for PPI networks among MMP-9 interactors, we found 1,814 PPI (out of 3,776) differentially co-expressed PPIs in at least one tissue-cancer dataset. Gained PPIs in tumour (tumour-specific PPIs) were defined as PPIs with $\rho_T > \rho_N$, and lost PPIs in tumour (normal-specific PPIs) were defined as PPIs with $\rho_N > \rho_T$. For significance of the number of differential PPIs across tissue-cancers, a binomial test was used to identify tissue-cancers in which the number of differential PPIs has been statistically significant. Expected probability of an interaction to be differential at each tissue-cancer was calculated by dividing the sum of differential

PPIs across all tissue-cancers by the total possibilities it may have across all tissue-cancers (i.e., the number of tissues multiplied by the size of the union of the differential PPIs). Heatmaps were generated heatmaps using gplots package (version 3.0.1) in R.

Data availability

TCGA KIRC RNA-seq datasets and associated clinical datasets are available at the cBioPortal for Cancer Genomics at http://gdac.broadinstitute.org/. Pan-cancer testing patient cohort GEO, the EGA and TCGA datasets are available at http://kmplot.com/. DEG protein profiles in cells and across 17 cancers are available from https://www.proteinatlas.org/. Transcriptomic datasets from melanoma and NSCLC patients treated with anti-PD-1 therapy are available from Hugo et al. (1), and Rizvi et al. (2). The HIV-1 elite controllers dataset is available from Zhang et al. (3), and the bacterial datasets are listed in Song et al. (4). Comprehensive pathway enrichment analysis and PPI analyses are available as Supplemental Data. The microarray data is published at the National Center for Biotechnology Information Gene Expression Omnibus (http://www.ncbi.nlm.nih.gov/geo) under GEO accession number GSE117230.

Code availability

R source codes used for: heatmaps, dendrograms, PCAs, prognostic genes identification from TCGA KIRC, synergistic prognostic genes identification from TCGA KIRC, and correlograms are available from the authors upon reasonable request.

Supplemental Methods References

1. Hugo W, Zaretsky JM, Sun L, Song C, Moreno BH, Hu-Lieskovan S, et al. Genomic and Transcriptomic Features of Response to Anti-PD-1 Therapy in Metastatic Melanoma. *Cell.* 2016;165(1):35-44.
2. Rizvi NA, Hellmann MD, Snyder A, Kvistborg P, Makarov V, Havel JJ, et al. Cancer immunology. Mutational landscape determines sensitivity to PD-1 blockade in non-small cell lung cancer. *Science.* 2015;348(6230):124-8.
3. Zhang LL, Zhang ZN, Wu X, Jiang YJ, Fu YJ, and Shang H. Transcriptomic meta-analysis identifies gene expression characteristics in various samples of HIV-infected patients with nonprogressive disease. *J Transl Med.* 2017;15(1):191.
4. Song F, Qian Y, Peng X, Li X, Xing P, Ye D, et al. The frontline of immune response in peripheral blood. *PLoS One.* 2017;12(8):e0182294.
5. Heberle H, Meirelles GV, da Silva FR, Telles GP, and Minghim R. InteractiVenn: a web-based tool for the analysis of sets through Venn diagrams. *BMC Bioinformatics.* 2015;16:169.
6. Rahmati S, Abovsky M, Pastrello C, and Jurisica I. pathDIP: an annotated resource for known and predicted human gene-pathway associations and pathway enrichment analysis. *Nucleic acids research.* 2017;45(D1):D419-D26.
7. Kotlyar M, Pastrello C, Malik Z, and Jurisica I. IID 2018 update: context-specific physical protein-protein interactions in human, model organisms and domesticated species. *Nucleic acids research.* 2018.
8. Brown KR, Otasek D, Ali M, McGuffin MJ, Xie W, Devani B, et al. NAViGaTOR: Network Analysis, Visualization and Graphing Toronto. *Bioinformatics.* 2009;25(24):3327-9.
9. Lim WK, Wang K, Lefebvre C, and Califano A. Comparative analysis of microarray normalization procedures: effects on reverse engineering gene networks. *Bioinformatics.* 2007;23(13):i282-8.